FİKRİ SEVEN

IZMIR KATIP CELEBI UNIVERSITY

IZMIR KATIP CELEBI UNIVERSITY
GRADUATE SCHOOL OF NATURAL AND APPLIED SCIENCES

DIELECTROPHORETICALLY ALIGNMENT OF MWCNTs IN POLY(ETHYLENE GLYCOL) DIMETHACRYLATE FOR NEURAL GUIDING OF PC12 CELLS

M.Sc. THESIS

Fikri SEVEN

Department of Biomedical Technologies

Thesis Advisor: Assoc. Prof. Dr. Mustafa ŞEN

JULY 2020

2020

IZMIR KATIP CELEBI UNIVERSITY
GRADUATE SCHOOL OF NATURAL AND APPLIED SCIENCES

DIELECTROPHORETICALLY ALIGNMENT OF MWCNTs IN POLY(ETHYLENE GLYCOL) DIMETHACRYLATE FOR NEURAL GUIDING OF PC12 CELLS

M.Sc. THESIS

Fikri SEVEN
(Y180204003)
ORCID: 0000-0003-1442-531X

Department of Biomedical Technologies

Thesis Advisor: Assoc. Prof. Dr. Mustafa ŞEN

JULY 2020

İZMİR KATİP CELEBİ ÜNİVERSİTESİ
FEN BİLİMLERİ ENSTİTÜSÜ

PC12 HÜCRELERİNİN NÖRAL YÖNLENDİRİLMESİ İÇİN ÇDKNT'LERİN POLİ(ETİLEN GLİKOL) DİMETAKRİLAT İÇİNDE DİELEKTROFORETİK OLARAK HİZALANMASI

YÜKSEK LİSANS TEZİ

Fikri SEVEN
(Y180204003)
ORCID: 0000-0003-1442-531X

Biyomedikal Teknolojiler Ana Bilim Dalı

Tez Danışmanı: Doç. Dr. Mustafa ŞEN

TEMMUZ 2020

Fikri SEVEN, a **M.Sc.** student of **IKCU Graduate School Of Natural And Applied Sciences**, successfully defended the thesis entitled "**DIELECTROPHORETICALLY ALIGNMENT OF MWCNTs IN POLY(ETHYLENE GLYCOL) DIMETHACRYLATE FOR NEURAL GUIDING OF PC12 CELLS**", which he prepared after fulfilling the requirements specified in the associated legislations, before the jury whose signatures are below.

Thesis Advisor :

Assoc. Prof. Dr. Mustafa ŞEN .....
İzmir Kâtip Çelebi University

Jury Members :

Asst. Prof. Dr. Ozan KARAMAN .....
İzmir Kâtip Çelebi University

Prof. Dr. Aydın AKAN .....
İzmir University of Economics

Date of Defense : 20/07/2020

To my family

FOREWORD

First and foremost, I would like to thank my advisor, Assoc. Prof. Dr. Mustafa Şen, for his great help, invaluable guidance and great support during my thesis and my university life.

I specially thank to Tansu Gölcez for her friendliness, collaboration and endless help during the experiments. It was pleasure for me to work with her.

I would like to thank to Ziyşan Buse Yaralı, Günnur Onak, and Gizem Dilara Ekimci for their help during my research work.

I am so thankful to Emel Bakay, Harun Hano, Kenan Ensarioğlu, and Gülsüm Ersu for their help, guidance and friendship.

I would like to express my love and gratitude to my family for their great support, and endless patience.

This thesis was supported by The Scientific and Technological Research Council of Turkey (TUBITAK) (Project No: 215E003).

July 2020

Fikri SEVEN

TABLE OF CONTENTS

Page

LIST OF FIGURES

Page

ABBREVIATIONS

PNS : Peripheral Nervous System

CNS : Central Nervous System

NGF : Nerve Growth Factor

PEGDMA : Poly(ethylene glycol) dimethacrylate

MWCNT : Multi Walled Carbon Nanotube

ITO : Indium Tin Oxide

DEP : Dielectrophoresis

AD : Alzheimer's disease

PD : Parkinson's disease

AFM : Atomic Force Microscopy

ALS : Amyotrophic lateral sclerosis

NT : Neurotrophins

BFCN : Basal Forebrain Cholinergic Neurons

PLL : Poly-L-lysine

PDMS : Poly(dimethyl) siloxane

CAD : Computer-Aided Design

PS : Polystyrene

PDL : Poly-D-lysine

HA : Hyaluronic acid

BMSC : Bone Marrow derived Mesenchymal Stem Cells

EDC : (1-Ethyl-N,N-dimethylaminopropyl carbodiimide)

BDNF : Brain-Derived Neurotrophic Factor

PLGA : Poly(lactic-co-glycolic acid)

PGA : Poly(glycolic acid)

PLA : Poly(lactic acid)

PEG : Poly(ethylene glycol)

pHEMA : Poly(2-hydroxyethyl methacrylate)

PA **:** Polyacrylamide

GelMA **:** Gelatin methacrylate

VEGF **:** Vascular Endothelial Growth Factor

NPC **:** Neural Progenitor Cell

NSC **:** Neural Stem Cell

MSC **:** Mesenchymal Stem Cell

HepG2 **:** Human hepatocellular carcinoma cells

HUVEC **:** Human Umbilical Vein Endothelial Cells

PIRE **:** Planar Interdigitated Ring Electrode

DHS **:** Donor Horse Serum

FBS **:** Fetal Bovine Serum

DMSO **:** Dimethyl sulfoxide

PBS **:** Phosphate Buffered Saline

TMSPM **:** 3-(Trimethoxysilyl) propyl methacrylate

PET **:** Polyethylene terephthalate

PCR **:** Polymerase Chain Reaction

DIELECTROPHORETICALLY ALIGNMENT OF MWCNTs IN POLY(ETHYLENE GLYCOL) DIMETHACRYLATE FOR NEURAL GUIDING OF PC12 CELLS

ABSTRACT

PC12 cell line is widely used as an in vitro model for neuronal diseases and studying cell differentiation behavior. The cell line has the ability to differentiate into neuron-like cells in the presence of nerve growth factor (NGF), resulting in neural extensions called dendrites and axons. Cell patterning is widely used in applications such as neuron network formation, tissue engineering, and cell based biosensors. In this study, the effect of randomly distributed and aligned multi walled carbon nanotubes (MWCNTs) in poly(ethylene glycol) dimethacrylate (PEGDMA) on PC12 cell neuronal differentiation behavior was investigated in the presence of NGF. First, the effect of randomly distributed MWCNTs in PEGDMA was investigated in terms of neurite length, number of neurite per cell and gene expression profiles of two neuronal differentiation markers. Then, an Au interdigitated electrode array (IDA) microchip was fabricated using contact-lithography. MWCNTs were aligned with dielectrophoresis in PEGDMA using the Au-IDA microchip and, UV treatment was used to polymerize the hydrogel, which helped fixing the position of aligned MWCNTs. The hydrogel containing the aligned MWCNTs was peeled off from the microchip and coated with collagen for PC12 cell seeding. The results clearly demonstrated that PC12 cells fell into microstructures created by the Au-IDA microchip and neurites followed the MWCNT tracks. The results of the study are expected to be useful for guiding neural growth in tissue engineering applications.

Keywords: Microchip, PC12 cells, MWCNTs, neuronal differentiation, dielectrophoresis.

PC12 HÜCRELERİNİN NÖRAL YÖNLENDİRİLMESİ İÇİN ÇDKNT'LERİN POLİ(ETİLEN GLİKOL) DİMETAKRİLAT İÇİNDE DİELEKTROFORETİK OLARAK HİZALANMASI

ÖZET

PC12 hücre hattı, nöral hastalıkları ve hücre farklılaşma davranışlarını incelemek için in vitro bir model olarak yaygın olarak kullanılmaktadır. Bu hücre hattı, sinir büyüme faktörü (NGF) varlığında farklılaşarak nörit, dentrit ve akson adı verilen uzantılar oluşturma yeteneğine sahiptir. Hücre desenleme; nöral ağ oluşumu, doku mühendisliği ve hücre bazlı biyosensörler gibi uygulamalarda yaygın olarak kullanılmaktadır. Bu çalışmada poli(etilen glikol) dimetakrilat (PEGDMA) içerisinde rastgele dağıtılmış ve hizalanmış çok duvarlı karbon nanotüplerin (ÇDKNT) NGF varlığında PC12 hücrelerinin farklılaşması üzerindeki etkileri araştırılmıştır. İlk olarak, PEGDMA içerisinde rastgele dağıtılmış ÇDKNT'lerin nöronal farklılaşma üzerindeki etkisi, nörit uzunluğu, hücre başına nörit sayısı ve iki nöronal farklılaşma belirtecinin ekspresyon profilleri açısından araştırılmıştır. Daha sonra, birbirine kenetlenmiş elektrot dizisine (IDA) sahip Au-mikroçip litografi yöntemiyle üretilmiştir. PEGDMA içerisinde süspanse edilen ÇDKNT'ler, Au-IDA mikroçip üzerinde dielektroforez uygulanarak hizalanmış ve daha sonra hidrojel, polimerizasyon için UV ışığına maruz bırakılmıştır. Hizalanmış ÇDKNT'leri içeren hidrojel mikroçip üzerinden ayırılmış ve PC12 hücrelerinin ekimi için kollajen ile kaplanmıştır. Sonuçlar, PC12 hücrelerinin Au-IDA mikroçipi ile oluşturulan mikroyapılara düştüğünü ve hizalanan ÇDKNT'lerin PC12 hücrelerinden uzanan nöritleri yönlendirdiğini açıkça göstermiştir. Çalışma sonuçlarının doku mühendisliği uygulamalarında nöral büyümenin yönlendirilmesinde yararlı olacağı düşünülmektedir.

Anahtar Kelimeler: Mikroçip, PC12 hücreleri, ÇDKNT, nöral farklılaşma, dielektroforez.

1. INTRODUCTION

1.1 Nervous System and Diseases

1.1.1 The nervous system

The nervous system consists of two main parts and these are peripheral nervous system (PNS) and central nervous system (CNS) (Figure 1.1). PNS and CNS together are responsible for somatic (sensorimotor or voluntary) and autonomic (involuntory) functions.The human CNS is the control panel for our bodies [1]. It is a network of more than 100 bilion individual nerve cells that responsible for cognitions, emotions, sense our surroundings, control our actions, and movements, briefly define who we are [2]. CNS is comprising the brain, spinal cord, and retina [3]. Brain consists of gray matter, including neuronal cell bodies, and white matter, including myelinated axons that form a network of interconnected neural circuits [4]. The spinal cord gets sensory information and controls the voluntary [1]. The third region of CNS is the retina which is the only part of the CNS that can be imagined directly [5]. The retina and optic nerve arise as outgrowth of developing brain in vertebrate embryonic development, and are responsible for detecting, processing, and sending visual information to the brain [6]. PNS provides the interaction of CNS with the environment and other organs. It contains two different regions named autonomic and somatic PNS. Somatic PNS is consists cranial nerves and spinal nerves, and autonomic PNS is composed of autonomic nerves and their respective ganglia [4].

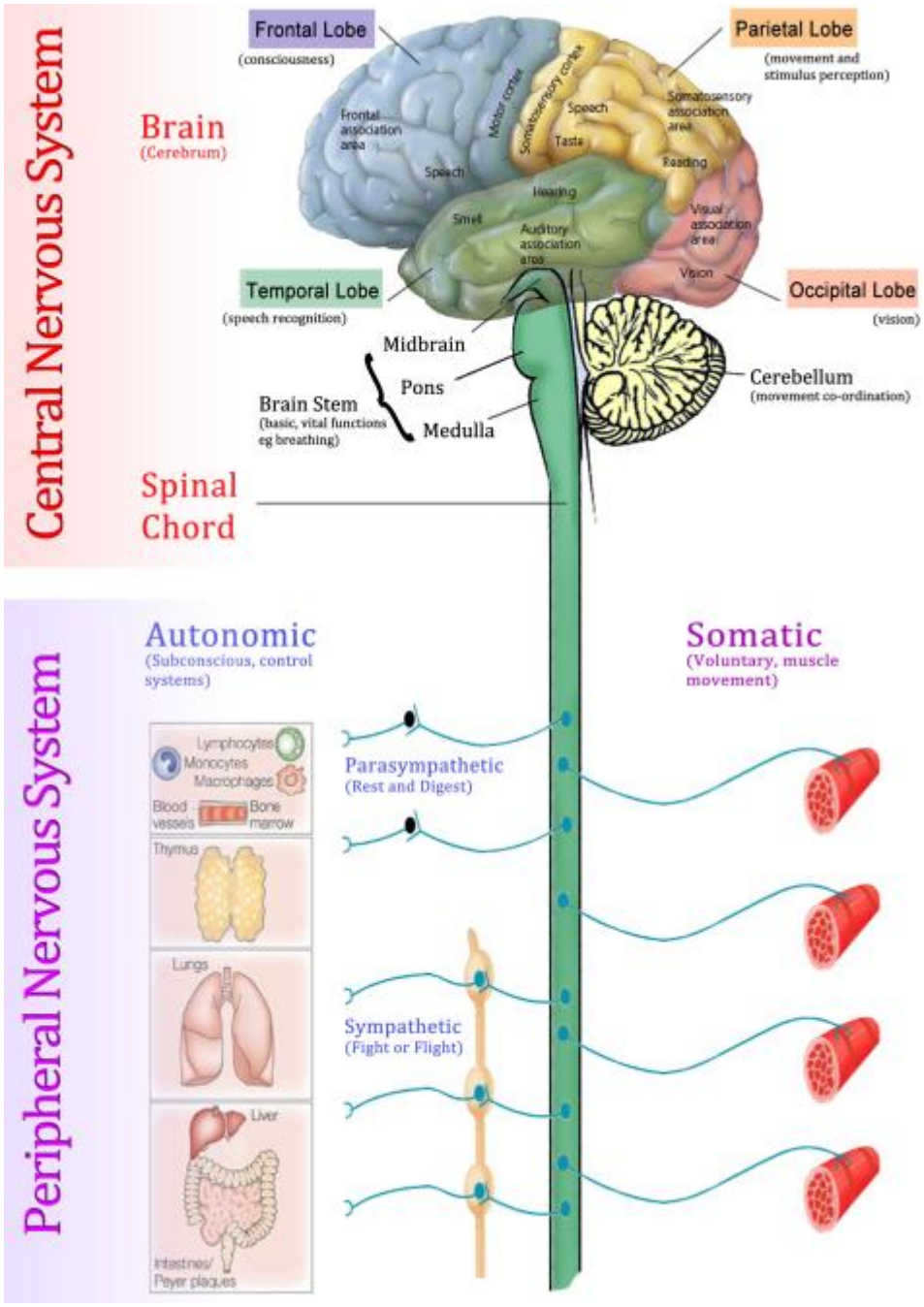

Figure 1.1. Major parts of the nervous system [7].

1.1.2 Functional components

Both PNS and CNS includes two basic types of cells: neurons that transmit and receive the chemical or electrical signals, and glial cells that process information to support functions for neurons. The neuron is the more important components of the two, with regard of its place for the communication of the nervous system. A human brain includes about 130 billion neurons with forming about 150 trillion synapses [8].

Neurons are the information-processing and transmitting elements of the nervous system and mainly contain the following parts: Cell body, axon, dendrites, and terminal buttons (Figure 1.2).

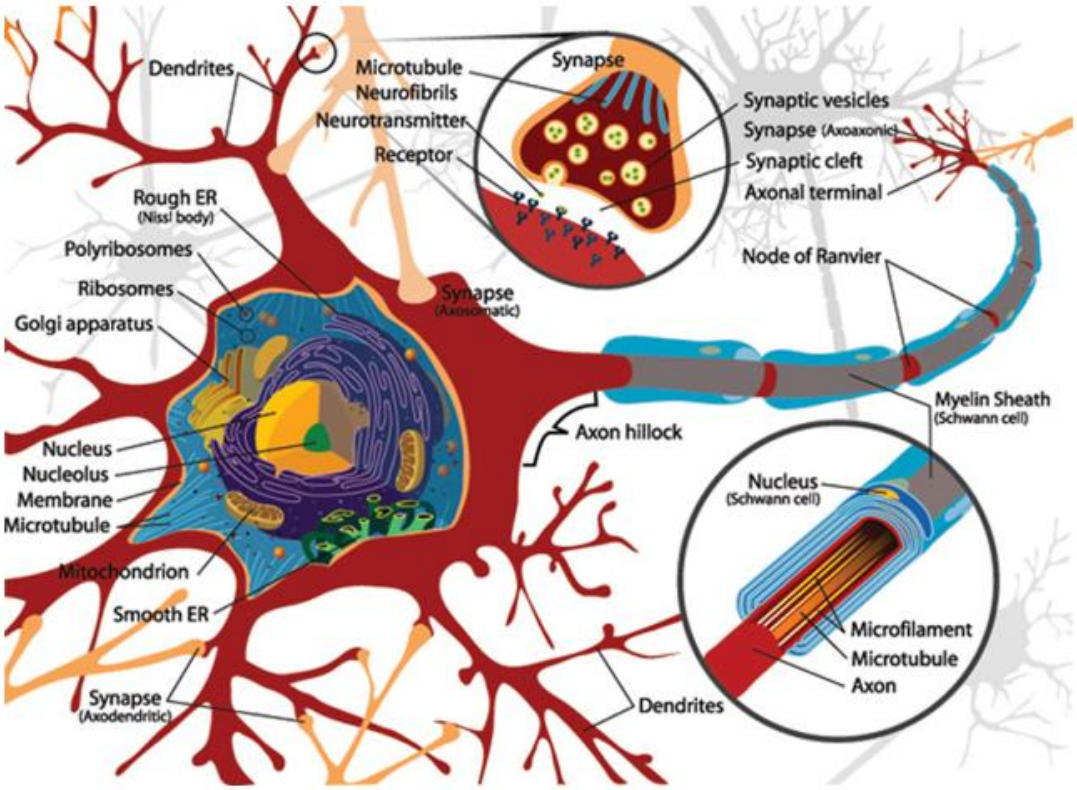

Figure 1.2. Neuron and its components [9].

Soma includes structures related to the vital processes of the nucleus and cell. Dendrites have a structure that branch off from the soma and responsible for receiving information from specialized junctions of other neurons named synapses. Axon is a thin cylindrical structure that transfers information from terminals to terminal buttons. Terminal buttons are button-like structures at the end of the axon branch; create synapses with another neuron and send information to that neuron [10, 11]. Cajal defined neurons as individual, polarized, functional components getting signals via root-like dendrites and transmitting outputs via the axon [12]. Single neuron doesn't act alone, neural communication relies on neurons connections that make with each other and with other cells. Dendrites from a single neuron can get synaptic link from many other neurons such as Purkinje cells that are thought to be connected with about 200,000 neurons [11]. The other type of cells called glia cells are non-neuron derived

cells that are responsible for the maintenance and protection of neurons (Figure 1.3). They are 5-10 times more in number in the CNS and PNS than neurons. The main glia cells of CNS are astrocytes, oligodendrocytes, microglia, and ependymal cells. Astrocytes perform many tasks in the CNS such as preventing the passage of harmful substances into the brain by creating a blood-brain barrier. It removes the neurotransmitters present in synapses with endocytosis. It provides pH and ion balances and mechanical support to neurons in the CNS [13]. Oligodendrocytes are responsible for creating a structure called myelin, which is composed of mainly lipid, in the axons of the neuron cells that make up the CNS. Since lipids make the axon membrane less permeable, in other words, it restricts the movement of ions, myelin accelerates signal transmission in the axon [14]. Ependymal cells are responsible for lining the ventricles around the brain that can be described as cavities [15]. Microglia cells are immune system cells and are responsible for protecting neurons in the CNS from pathogens. They proliferate quickly following the injury of CNS and create the essential neuroinflammatory markers for neural regeneration [16]. PNS's basic glia cells are satellite cells and Schwann cells. Schwann cells are also responsible for wrapping around the axons of neurons with lipids, in other words, forming myelin like oligodendrocytes. But, an oligodendrocyte can myelinate multiple neurons, while a Schwann cell can myelinate only one neuron [17]. Satellite cells are located around the neurons that make up the PNS, and provide them mechanical support and regulate their microenvironment [18].

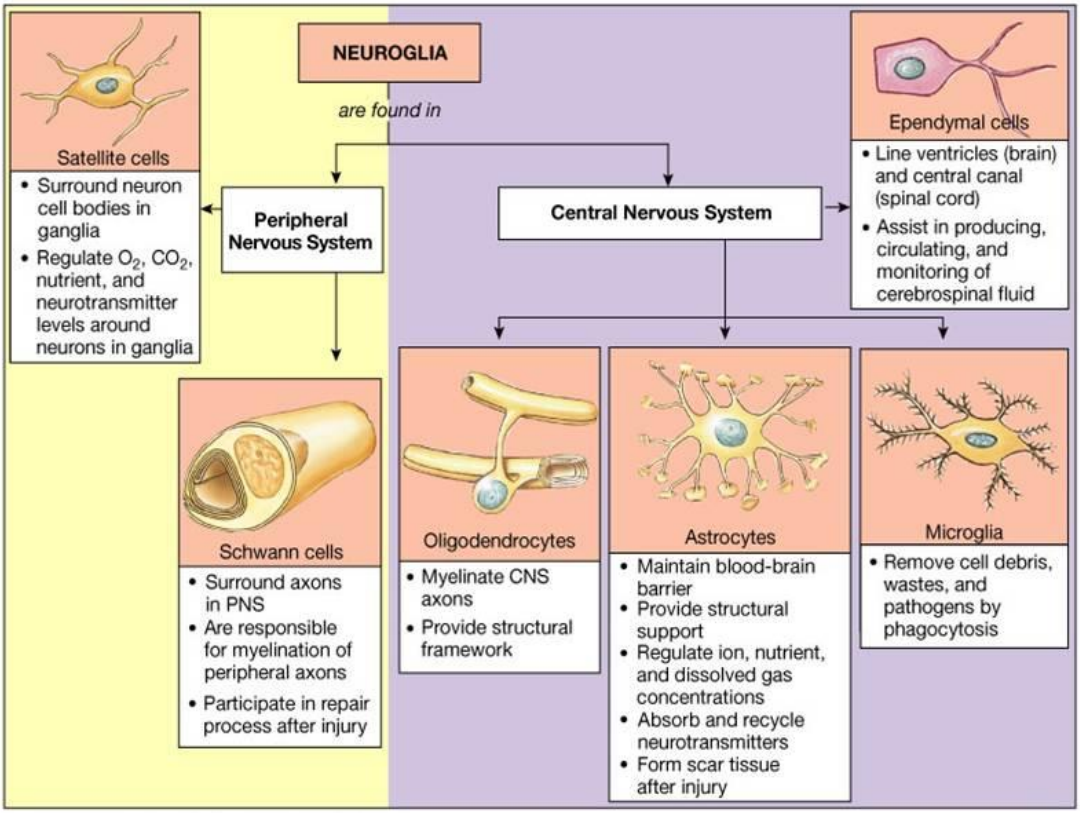

Figure 1.3. Types of neuroglias found in PNS and CNS [19]**.**

1.1.3 The nervous system diseases and nerve regeneration

Diseases of nervous system are criticaly affect body health. Injuries of central and peripheral nervous system or harm to nerve cells may trigger severe nervous system diseases. Neurodegenerative diseases are the results of loss of functions in the brain, spinal cord and nerve cells [20]. When the loss of function or damage occurs in CNS or PNS, anyone may have problem for some functions as shaking, moving, or learning and also some problems with memory [9]. In some sections of the brain, gathering of nonsoluble filamentous aggregates in some parts of the brain is the main causes of neurodegenerative diseases. It mostly results with inflammatory damage and cell death at the accumulation areas. These aggregates creates patterns which are special for each individual disorder [21]. Neurodegenerative diseases affect millions of people in the world. There are more than 600 neurological disease and among them Parkinson's disease (PD) and Alzheimer’s disease (AD) are the most general ones (Figure 1.4) [22]. The risk of being affected by neurodegenerative diseases is increasing with the increase in aged population and these diseases are becoming more common due to

increased life expectancy and changing population demographics [23, 24]. The medical condition that develops in the form of memory loss (dementia) and decreased cognitive functions in general due to the death of brain cells over time is called AD. It is the broadest type of dementia. In the initial phase, the disease manifests itself only with simple forgetfulness, and it can progress until the patient forgets about the events that are experienced in the past and fails to recognize the family members. Also diminishing of language skills, movement and decision-making abilities can be observed [9]. These effects result from amyloid plaques that trigger to increasing of oxidative stress and neuroinflammation [25]. The reason for AD development could'nt been established for years despite the many scientific studies. However, the potential reasons that are thought as risk factors in the development of the disease are advanced age, family history of AD, sleep disorders, past brain injury incident, high blood pressure and high cholesterol [26]. Reason of PD development is the death of cells that produce the dopamine which is a neurotransmitter in the brain that provide nerve cells communication and also associated with Lewy bodies (unusual aggregations of protein that develop inside nerve cells) formation due to the alpha-synuclein proteins activation and phosphorylation [25]. The cells producing dopamine are managing the control, fluency, and placement of movements [27]. Symptoms of PD can be divided into groups and differed in each patient [28].

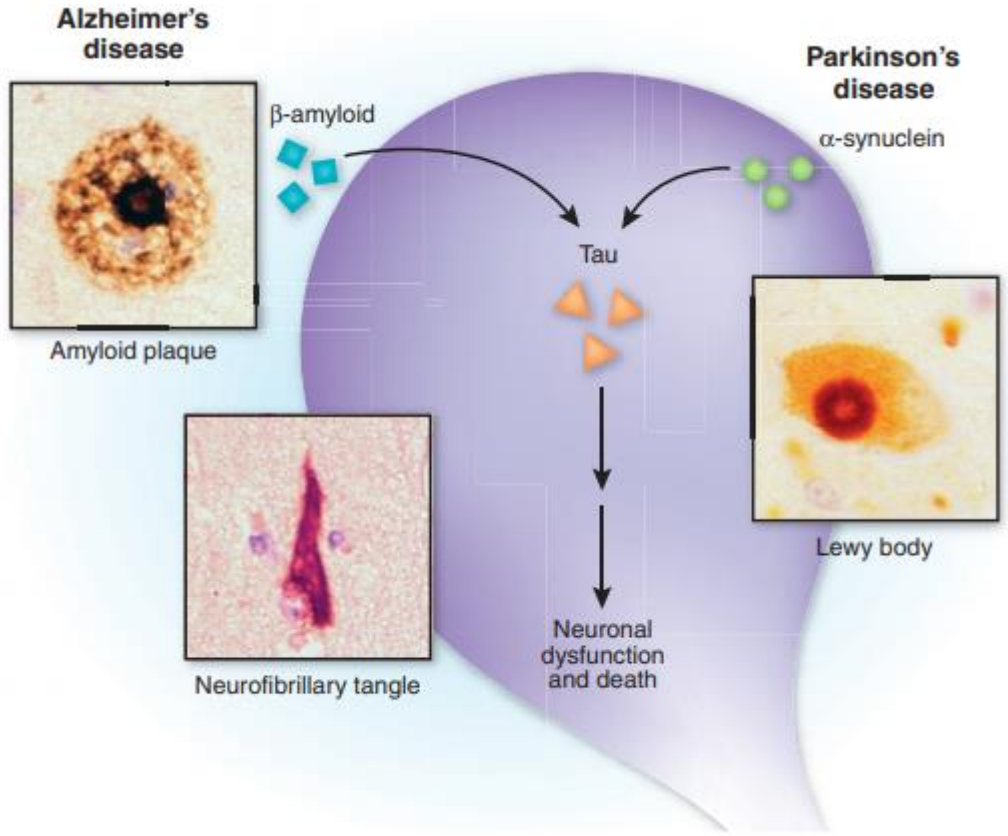

Figure 1.4. Most common diseases AD and PD, and their causes [29].

Amyotrophic lateral sclerosis (ALS) (deterioration of nerves slowly), brain and spinal cord injuries, Huntington's disease, multiple sclerosis, and schizophrenia are the some of other neurodegenerative diseases [9]. PNS injuries are mostly classified with Seddon and Sunderland classification. Seddon classification which was defined in 1942 divides injuries to three groups: axonotmesis, neurapraxia and neurotmesis (Figure 1.5) [30]. Neurapraxia is a temporary damage that does not disrupt axonal integrity, but there is a physiological barrier in this damage that affects axons in nerve conduction. In axonotmesis, the axons in the nerve cell to be interrupted, but there is no connective tissue damage. Neurotmesis is loss of nerve integrity by damaging both axons and connective tissue [31].

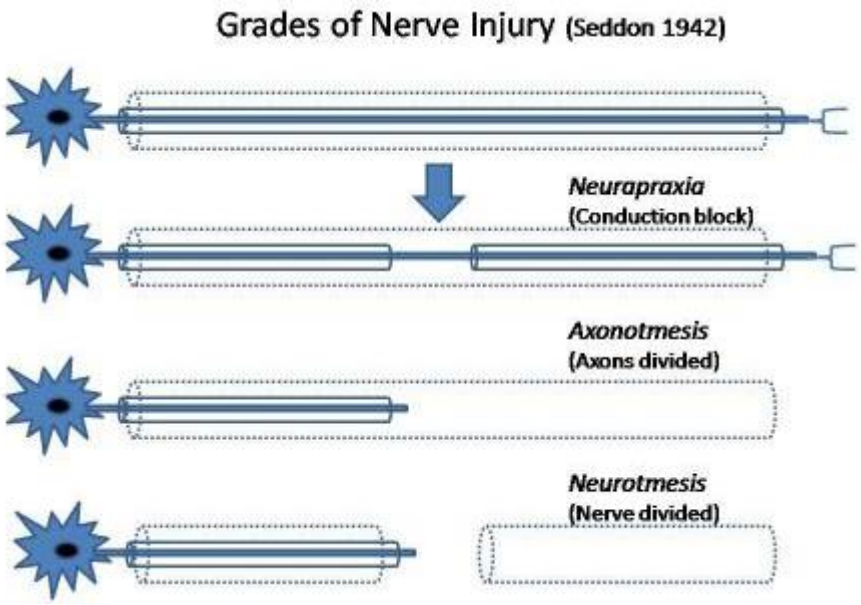

Figure 1.5. Seddon classification [32].

Worldwide, in 2015 there are about 46 million people were suffering with neurodegenerative diseases and their debilitating nature makes the diseases leading cause of dependence and disability [33]. About $800 billion is spent each year just in the U.S. [34] which is a huge economic burden. Since there is a huge economic burden and many people that have neurodegenerative diseases, regenerative therapies are urgently needed to healing of the neurological functions. In the regeneration of nervous system, extracellular factors are mostly significative factors, therefore the role of environmental factors on neural regeneration such as neurotrophic factors and extracellular matrix components of nerve cells must be well understood to use proper material with well therapeutic effect at the injury site.

1.2 Nerve Growth Factor and Nervous System Degeneration

Nerve growth factor (NGF) is one of the first explored members of the neurotrophin family. Neurotrophins (NT) are essential to sustain synaptic function control, neural life morphology, plasticity, and differentiation in adult nervous system. NGF is described as a trophic (growth) protein with message-receiver role between tissue that reacts against dorsal root ganglion maturation, axonal growth, neuroblast proliferation, peripheral stimulation and nerves that stimulate tissue [35]. NGF was firstly isolated by Stanley Cihan and Rita Levi-Montalcini in 1956, but it wasn't broadly known, until

it won the Nobel Prize in 1986 in the subject of Physiology or Medicine. The finding of NGF started with the interest of Rita Levi-Montalcini about the supposition that a diffusible agent that released from transplanted tumor tissues induced differentiation and growth of nerve cells. Further investigations provided that tumor could release a diffusible agent that supported neurite outgrowth and induced nerve cell differentiation in a dose-dependent manner [36]. After she collaborated with Stanley Cohen, they performed experiments to identify this diffusible factor if it is a nucleic acid or protein. They utilized snake venom to crush nucleic acids. Shockingly, they saw that snake venom empowered the nerve cells to broaden more neurites than non-envenomed cell cultures. The evidences of the particle in snake venom drove Cohen to believe importance of investigating the mammalian sample that has similarity with gland of snake venom. Then, he proceeded with gland of mouse salivary. Then, they found that this gland is rich with this particle, and diffusible factor too. They succeeded to isolate this molecule and showed that it was a protein [37, 38]. Because this protein which was then called Nerve Growth Factor, could be isolated in large quantities from mouse salivary glands. They can show the impotance of NGF for sensory ganglia growth in vivo investigations and could make antibodies against NGF [39].

NGF is also known as a pleiotropic (having multiple phenotypic expression) factor with activities beside nervous system. It is made and used by some cell types, such as structural (endothelial and epithelial cells, hepatocytes, etc.), immune (lymphocytes, mast cells, granulocytes, antigen presenting cells), and accessory (Muller cells, glial cells and astrocytes) cells [40, 41] (Figure 1.6). NGF gained great charm with its discovery for its potential applications in varied fields, especially in the treatment of neural diseases and also as treating-supporting agent in the ulcer control [42]. The healing effects of NGF were studied and it showed remarkable results in impaired healing because of autoimmune disorders or experimental injury. Besides the human pressure and cutaneous ulcers, successful effects were obtained during local long-term NGF applications [43-45]. In vitro studies also showed that fibroblasts are the target cells for the NGF-driven healing [46] and many patients with corneal ulcers because of neurotrophic corruptions related with chemical burns, local surgery, herpetic infections, and diabetes have been treated so far [47, 42].

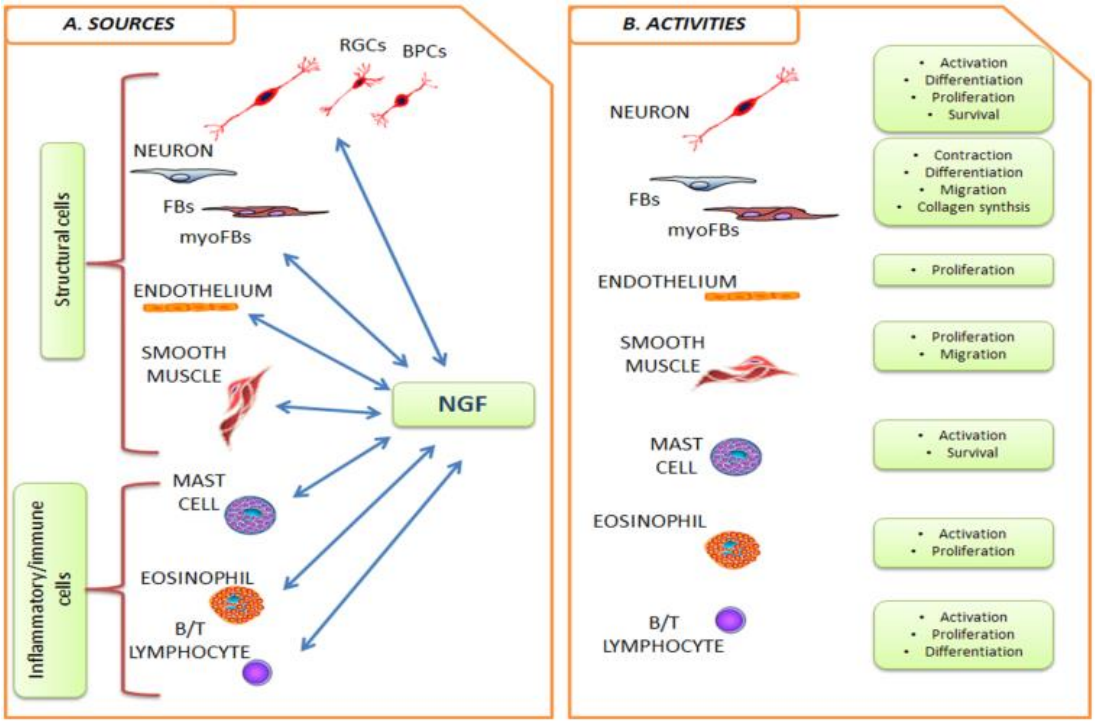

Figure 1.6. NGF target cells. Cell types of nervous and immune system and producers of NGF (A), and functional activities of these cells (B) [48].

Studies on animals and isolated cells showed that NGF has protective action on the control of neurotransmitters and neuropeptides synthesis of sympathetic and sensory nerve cells besides on the survival of degenerating peripheral nerve cells [49, 50]. While exogenous NGF management affects neural plasticity which provides altering adult nervous system functions and structure with cause of stimuli [50]. In vivo down-regulation of NGF through the management of NGF-antibodies or by peripheral nerve wound causes a remarkable decrease in Substance P and Calcitonin-Gene Related Peptide synthesis. In adult tissues, constructive synthesis of NGF is related with PNS neurons phenotypic properties including , dendrites arborization, cell body size, axonal terminal sprouting, induction and inhibition of neurotransmitters, and neuropeptides [51].

CNS diseases are defined as the progressive loss of structure and functions of neurons, mostly due to result of not enough synthesis or release of neurotrophic factors like NGF [52]. While exogenous management of NGF could protect degenerating neurons, synthesis or release of NGF and NGF signaling of brain were significantly influenced in brain diseases [53]. Studies showed that NGF can support Basal Forebrain

Cholinergic Neurons (BFCN) survival which is characterized to degenerate in AD like diseases relating age. Studies showed that intracerebral management of NGF may reduce or prevent brain neuronal degeneration of AD patients. Experiments in the 1980's demonstrated that intracerebral management of NGF was able to prevent the wound-induced degeneration of BFCN in animal experiments and delay the atrophy in the elderly rat brain neurons [54, 55]. After a few years, testing of NGF in AD patients was resulted with weight loss, systemic pain and only mild neurological healings [56, 57]. In the 1990s, strategies for the delivery of NGF into the damaged brain neurons and to bypass safely the Brain-Blood-Barrier was identified [58]. Studies demonstrated that nose-to-brain path may be a potential useful and safe path for targeting drugs to the brain via the olfactory pathway [59, 60]. Nose-brain and eye-brain routes have been studied by different groups to show the potential alternative pathway of delivering NGF into the brain. Chen *et al.* made the first demonstration of safely NGF delivery to damaged brain neurons. They demonstrated that NGF managed by nasal cavity can protect the damaged BFCN and improves the behavioral performance in AD experimental models [59]. Also another study demonstrated that eye local NGF management can reach damaged brain neurons and protect them and support behavior performance [61].

1.3 Cell Patterning

Cells are cultured on homogenous substrates and getting beneficial information about cellular behavior ad signal transduction is hard. Cells need special administration for the applications like cell based biosensor, tissue engineering, and prosthetic. Cell patterning can provide these control over the cell which is basically described. Cell patterning has been widely used for investigating the biocompatibility of varied substrates, obtain administration neurite outgrowth, regulate polarity in neurites, and improve tissue engineering and their applications [62]. It can be utilized to control cell-cell interactions, modifying the contact area between two cell types in co-culture [63], and also to direct cell-matrix interactions, with manipulating the amount of contact area with extracellular matrix (ECM) [64] or type of ECM that the cells placed on [65]. Cell patterning also can be used to enhance cell-based biosensors with utilizing living cells as sensing components for the applications such as toxin detection [66] and

defense monitoring [67] and recent advances in cell patterning can allow production of reproducible and manufacturable biosensor devices [68]. Several different approaches were made for cell patterning applications so far.

One of the cell patterning method is inkjet printing. Traditional inkjet printers pattern pigments by depositing droplets in micrometer sized diameters under robotic control and same principle can be utilized to pattern cell-adhesive substance as collagen or poly-L-lysine (PLL) onto a cell-repellant background or to print droplets of biological substances containing living cells with high sensitivity [69]. Roth and his collaborates printed collagen with utilizing a conventional inkjet printer with shapes containing dot arrays, lines, and gradients to pattern smooth muscle cells derived from rat aorta [70]. They cultured the cells on the patterned surface and the technique allowed the formation of living cellular patterns with a resolution of 350 μm. Also in another study, cell-loaded hydrogel tubes with submillimeter diameter were produced where the cell-loaded alginate gel prepared to produce a tubular structure. Also cell-loaded fibrin patterns were printed via depositing droplets of cell-loaded fibrinogen solution in solution. Inkjet-printing methods also used for biosensor development, free-form fabrication methods to make polymeric scaffolds, DNA arrays, also for patterning hippocampal rat neurons and glia (Figure 1.7) [71]. The inkjet-printing method is relatively cheap, repeatable, flexible and has high output, but the resolution is limited to about 10 μm and only specific materials can be printed.

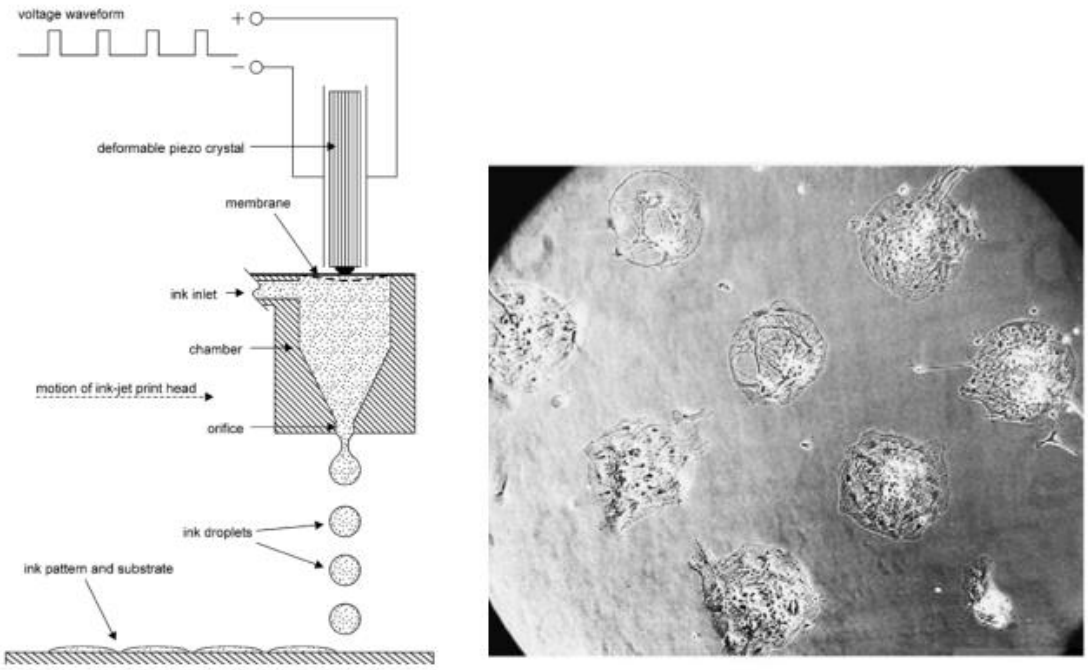

Figure 1.7. Left: Illustration of the processing of an ink-jet print head. Droplets with 10-100 μm in diameter take a ballistic trajectory onto the glass substrate. The print head moves robotically as droplets are ejected. Right: rat hippocampal cells adhering to 350 μm diameter printed patterns including micro-islands of collagen/PDL after 8 days [71].

In microcontact printing method, biosubstance are inked onto a patterned elastomeric stamp and then stamped onto the wanted substrate, then transferred [72]. Elastomeric stamp is fabricated with firstly coating of silicon with photoresist that created as patterns. Then, liquid phase hydrogel like poly (dimethyl) siloxane (PDMS) was implemented to photoresist for fabrication of stamp. After curing, stamp is inked with cell-adhesive (cytophilic) proteins like fibronectin and implemented in a certain surface [73]. The method is utilized by different inking molecules and cell types such as keratocytes and fibroblasts [74]. Belkaid *et al.* utilized this method using PDMS stamps inked with PLL and printed onto the coverslips to pattern neuronal cells including hippocampal and cortical cells on linear and octagonal patterns (Figure 1.8) [75]. Microcontact printing is principally simple and flexible. However, it has problems such as pattern degradation after a while due to protein denaturation and it is difficult to align stamp when it comes to using with micro-sized components.

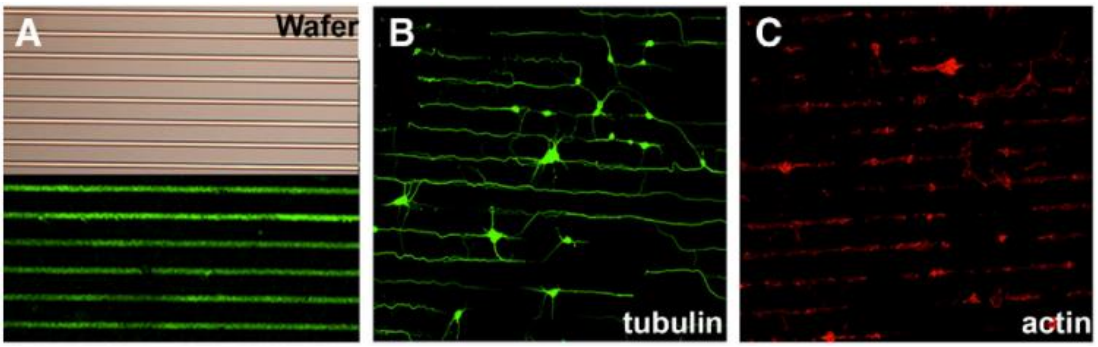

Figure 1.8. Microcontact printing study for guiding neuronal morphogenesis. A: (top) silicon master with 10 μm thick lines separated by a pitch of 60 μm, (bottom) uFITC-conjugated PLL lines printed onto coverglass. B:Primary hippocampal neurons plated on micropatterned PLL and immuno-stained for neuron-specific β-3 tubulin. C: Primary cortical neurons plated on micro-patterned PLL and stained for F-actin [75].

Physical immobilization methods varied from fabrication of three-dimensional (3D) structures like pillars or compounds to catch cell bodies, to changing of surface topography or roughness to modify adhesion properties. Zeck *et al.* immobilized the individual neurons from snail using a microscopic 'picket fence' of polyimide on a semiconductor chip [76]. These physically restricted cells created a network with post-synaptic stimulation regulating the current of an on-chip transistor. Also in another study, a similar principle was used to decrease neuronal migration on patterned substrates with utilizing arrays of vertical nanopillars that formed by ion beam platinum deposition (Figure 1.9) [77]. The movement of neurons on the nanopillars were restrained. The physical immobilization methods mostly don't depend short-lived chemical cues activation or biological elements, but they have complex and expensive fabrication processes especially for the microscale surfaces and the control of neurite action is restricted.

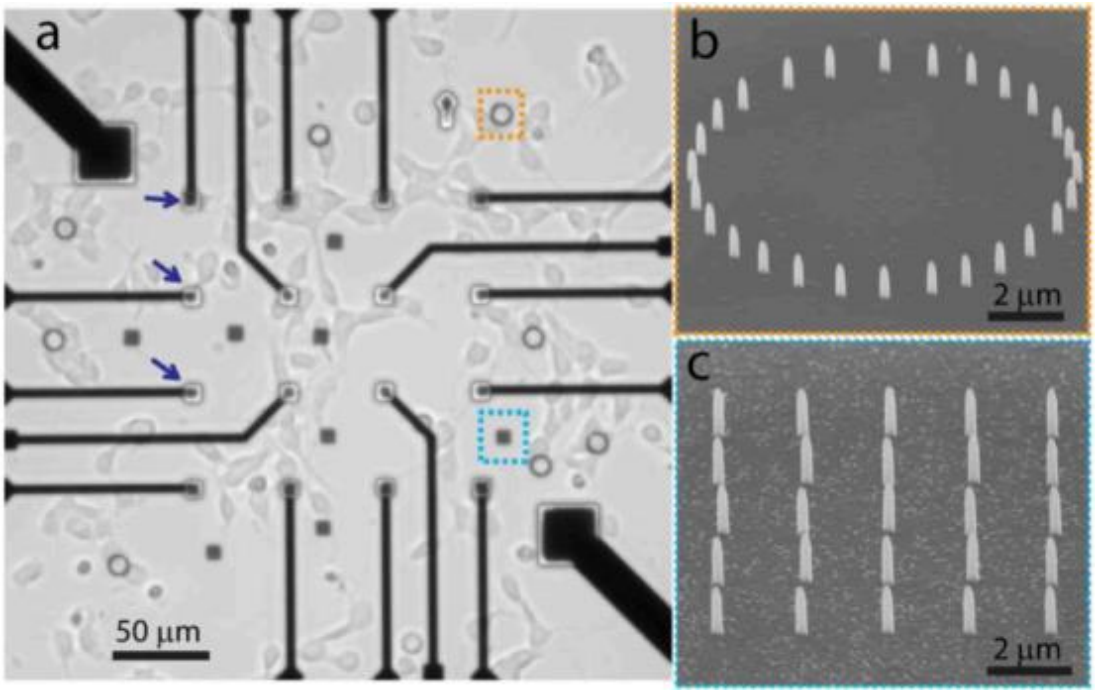

Figure 1.9. Cultured neurons on a nanopillar substrate to limit their migration. A: Bright field image of neurons on MEA substrate with nanopillar arrays located both on the microelectrodes (blue arrows) and in open areas (orange and cyan squares). B: SEM image of ring-shaped nanopillar array. C: SEM image of 5×5 square nanopillar array [77].

Another method for patterning includes the changing the adhesive behavior of the different substrate surfaces more cunningly. Dowell-Mesfin and collaborates discovered the effect of certain murine hippocampal neurons topographical cues (Figure 1.10) [78]. Nerve cells were grown on surfaces that PLL coated with 1 µm high and varied width formed by photolithographic methods. Neurite outgrowth on smooth surfaces was random, but on areas with pillars, the neurons showed more orthogonal growth. Carbon nanotubes (CNT) with their special electrical, mechanical, chemical and surface characteristics have great potential for the harnessing control of neuronal adhesion [79]. In a study 20 µm CNT islands on quartz grounds were used for culturing neurons on [80]. They discovered that neurons preferred to attach on the rough-textured CNT islands with processes entwined and curled between the CNTs. The results showed that a mechanical effect like entanglement, can create an extra mechanism by which neurons or other cell types force themselves to nano-roughened surfaces.

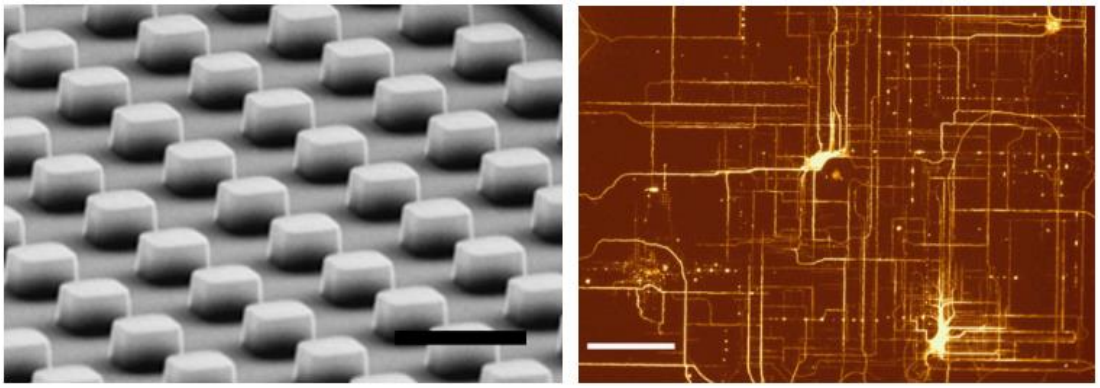

Figure 1.10. Left: SEM image of an array of pillars with 1 μm height (Scale bar 4 μm). Right: Automated tracing of β-3 tubulin-labelled rat hippocampal neurons grown on the pillar array. Note the vertical growth pattern of neurites (Scale bar 100 μm) [78].

Photolithography is the process of transferring the geometric shapes of a pre-prepared mask to the photoresist coated substrates like silicon wafer by illumination like ultraviolet light mostly [81]. The word lithography derived from Ancient Greek word lithos meaning stone and graphein meaning to write. It was known as the art of printing of figures and writings drawn in oily ink on limestone [82]. The photolithography is the mostly preferred lithography method. In photolithography process, firstly a photomask is designed using a suitable computer program like Vectorworks or computer-aided design (CAD) and produced on a quartz covered with a tiny layer of opaque chromium that includes the desired geometric pattern with allowing sub-micron resolution. A UV-sensitive polymer called photoresist firstly coated on the substrate to be patterned. After polymerization of coating material, it is aligned and came into contact with the mask. Then, UV-light is applied from a UV-source to the unprotected areas of photoresist. Therefore, the irradiated areas become soluble and removable in a following development step (with positive photoresist mentality in which the UV-irradiation weakens the polymer) or the irradiated areas become insoluble for development step so the unexposed areas can be removed (with negative photoresist mentality in which the UV-irradiation strengthen the polymer) with leaving the representation of the photomask pattern behind [81]. This method has a long history of which started in the 1820s, with the invention of a photographic process by Nicephore Niepce that used a natural asphalt called Bitumen of Judea as the first photoresist [83]. The method is widely used in the production of semiconductor

devices where silicon dioxide wafers are mostly utilized as a substrate. The technology has utilized for cell patterning with varied forms. For example, Scotchford *et al.* created micro patterns with varied metal oxides including aluminum, niobium, titanium, and vanadium (Figure 1.11) [84].

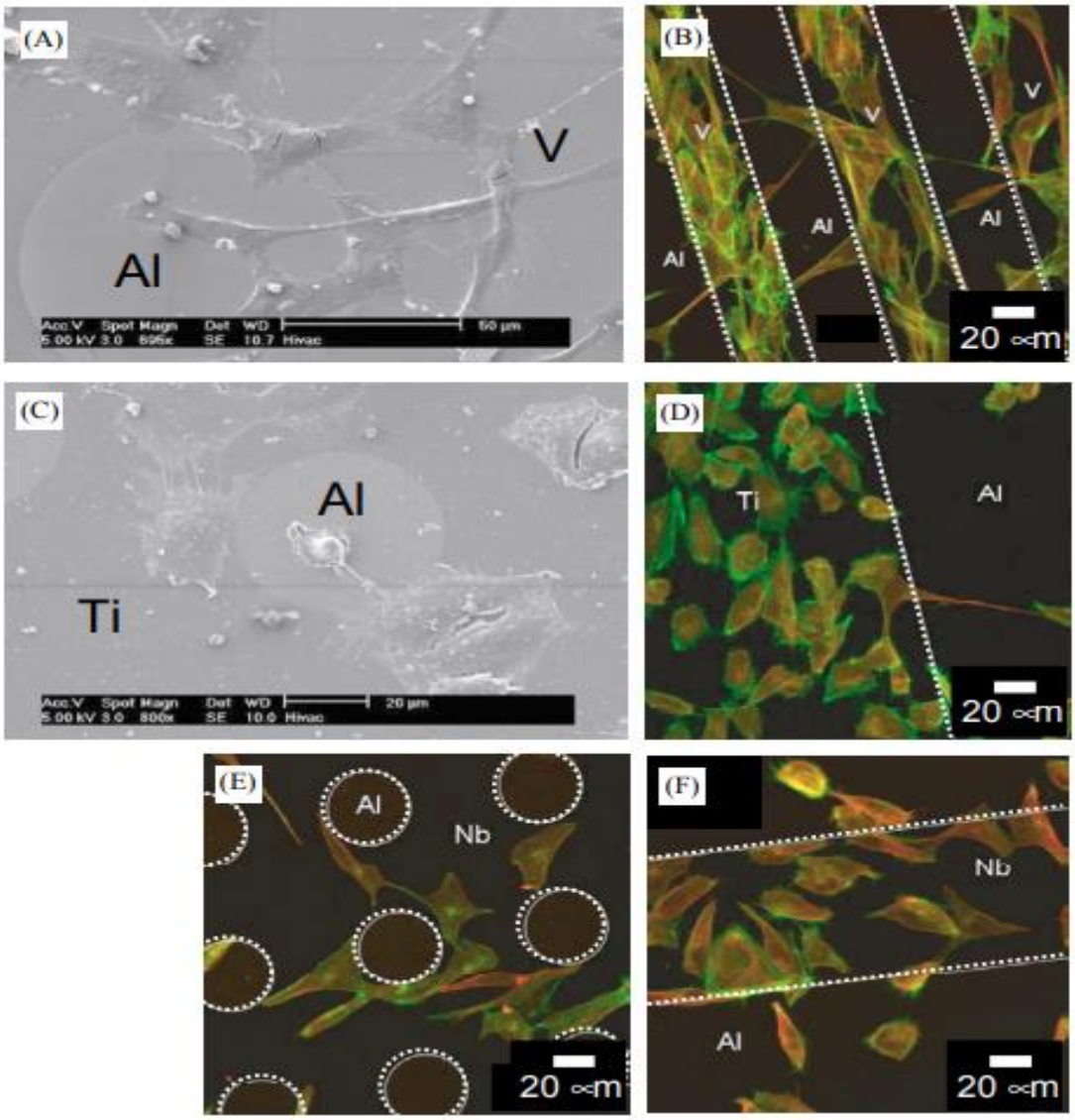

Figure 1.11. SEM and confocal micrographs images of cells cultured on varied patterned surfaces for 18 h. The confocal images show the f-actin (green) and microtubule skeletons (red). All data suggest that cells prefere to avoid adherence on Al. This holds for such patterns with (A) and (B) Al/V; (C) and (D) Al/Ti and (E) and (F) Al/Nb surfaces (only confocal data is shown for this bimetal combination) [84].

The cells recognized the differences between these metals and demonstrated differential surface adhesion and migration behaviors. Their preference was related

with and increased concentration of bound fibronectin for the surfaces composed of titanium, niobium and vanadium metal oxides.

Microfluidics tackles with the attitude, management, and manipulation of fluids at submillimeter scale. The substances like PDMS are utilized to form a network of 3D channels for cell patterning [85]. Morin and collaborates associated a 3D PDMS structure with a planar microelectrode array [86]. The microfluidics technique has potential for the targeted pharmacological therapy with controlling the liquid environment.

Another technique called real-time manipulation deals with dynamically changing the position and growth of cells in culture real-time such as the utilization of extracellular direct current across a culture. Kim and collaborates used galvanotaxis to control the behavior of a eukaryotic ciliate called *Tetrahymena pyriformis* [87]. They managed to guide a cell in a desired direction at a microchannel intersection by changing a 2D electric field formed utilizing four electrodes with the advantage of a behavioral response named cathodal galvanotaxis. In this technique advanced extra apparatus and real-time cues are required to be used continuously to the culture.

1.4 Neural Guiding

1.4.1 Disease modeling

Engineered neural networks can provide understanding for the complex neuropathological processes. In neurological diseases like AD [88] and epilepsy [89], alterations in network connectivity have been defined. But, engineered networks can provide the best benefit in trials to understand neuropsychiatric disorders. In the control of either depression or schizophrenia, there has not been remarkable progress compare to other areas of medicine recently. One of the reason is deep unawareness of the primary pathophysiology and anatomical regions of disease. There is an increasing concurrence that diseases containing schizophrenia, mood disorders, and autism might demonstrate ‘connectopathies’ [90] which represent as a result of abnormal connectivity.

For getting the desired effect in brain disease modeling, mainly two different mechanistic modeling attempts are considered: preventive and curative treatment. The

preventive attempt needs to define predictive biomarkers and the causal factors that cause the conversion of healthy network to pathological one. The curative attempt contains healing the system or managing the symptoms. The mechanism for the targeted attempts or the mechanism of co-morbidities doesn't need to be same to those of the underlying pathology that refers the requirement to define multiple therapeutic targets. Most of the neurological diseases include multiple interconnected brain regions identifying a network problem. The problem must be considered at least at the organ level like the whole brain, because a damaged small area can have large-scale reactions affecting whole brain functions. Most of the pathological cases are related with metabolic malfunction, an altered connectome, and changed whole brain dynamics, but these findings are hard to solve due to absence of conceptual framework to evaluate them. It is hard to understand if these changes are associated with biomarkers or pathology/symptoms, or a result of pathological continuum [91]. When planning the model neural disease, the first and the most important step is to make a decision for the private cell model required for this study. This step contains deciding starting material and required some steps and nerve cells [92].

Neural network engineering with these attempts provides an attractive disease modelling chance. Modelling the disease as in vitro networks like cell patterning also offers a chance to use recent experimental interventions that cannot be applicable in vivo.

1.4.2 PC12 cell line

PC12 cells were established as a clonal cell line derived from an induced, transplantable rat pheochromocytoma, adrenal medullary tumor which firstly cultured by Greene and Tischler in 1976. After its derivation, this cell line was broadly used for varied studies including mostly neuronal and endocrine cell physiology. When, they preserved in growth medium, the cells proliferate and resemble to their chromaffin cell counterparts. They can be synthesized, stored and induced to release catecholamines [93]. Differentiation of PC12 cells into a neuronal phenotype which means restriction of proliferation and starting of neurite outgrowth by NGF treatment was represented in the first report on the cells, and countless following studies of neurotrophin signaling were presented using this cell line [94, 95]. The differentiated cells are in phenotype

look like sympathetic neurons. They prolong branched axons and can transmit signals along them, become electrically inducible, and responsive to neurotransmitters, enounce a high range of neuronal markers and keep their capacity for dopamine synthesis, uptake, release, and storage.

In laboratory circumstances, attachment of PC12 cells to polystyrene (PS) tissue culture surfaces is weak, and they grow mostly as floating cell clusters on these surfaces. This situation mostly results with inadequate levels of neurite outgrowth. To enhance the attachment of the PC12 cells, surface functionalization is used. It was demonstrated that treatment of surface with proteins before culturing like ECM components, improved cell growth, migration, morphology, and differentiation as well as cell adhesion with rising their life-span. Various types of coatings were presented in the studies including collagen, glycoproteins, laminin, fibronectin, poly-D-lysine (PDL), and PLL to improve attachment of PC12 cells [96].

PC12 cells provide general advantages to the studies with their capability of limitless proliferation. They may be cultivated in high amounts with a minimum endeavor. Since they are reproduced from a single progenitor, they show homogenous population in some degree that can be utilized to supply duplicate cultures. With these properties, they are broadly utilized for defining environmental elements which can cause PD. These cells also can be genetically altered by viral or transfection infection. Their modified sublines can be picked and multiplied. These features are precious for probing the molecular features of cell death and for forming and characterizing genetic models of neural diseases. Another property of this cell line is allowing the very fast experimentation. Most of the utilized cell lines as PD models cause degeneration of neurons and death in 2 days. Genetic management by gene overexpression is possible in a short time. The cell line has been utilized over thousands of studies with its features and gene expression patterns, mostly as a model for defining neurons behaviors and answering diverse range of stresses. Its popularity increases. The neural differentiation capability of PC12 cells in response to NGF is a beneficial and critical property. It provides possibility to create high numbers of cells to transform the population to a post-mitotic condition with many of the properties of sympathetic and dopaminergic neurons. The neutrally differentiated cells has advantage to utilize them as model sympathetic neurons that affected by the neural diseases. Their responses to NGF and

other neurotrophic factors offer chances to know the mechanism that growth factors induce neuroprotection in neural diseases [97]. Neural differentiation of PC12 cells is evaluated by quantitative or semi-quantitative morphological methods containing the measurement of the cell size, neurite number and neurite length. And this feature of cells are broadly used as a neuron cell model in neuroscience for both neurobiological and neurotoxicological studies as a model such as injury-excited neuropathic pain model, nitric oxide-excited neurotoxicity model [98].

1.4.3 Importance of neural guiding

In vivo, well-organized genetic programs allow neural cell bodies for placing rightly, create convenient routes to reach exact destination. In the formation of complex structure of brain which is principle organ of the human nervous system, neural network and synapse formation have primary role. The brain, like other organs, has the ability to grow in size and become more complex in function and structure by migration of different types of cells to specific regions. Cell migration has a significant effect on intercellular synapse formation and these two events develop depending on the stimulating molecules in the environment [99]. After leaving the epithelium covering the ventricular space, which can reproduce, the neurons migrate in two different directions, mainly circular and angular [100]. In circular migration, neurons move through the circular glial fibers perpendicular to the ventricular space, allowing the neural tube to thicken. In angular migration, neuron cells migrate parallel to the ventricular space. Thus, the brain continues to grow in size. In order for the brain to be functional, these migrating cells must interact with other at their destination and form synapses. Neurons create the dendrites and axon structures to exchange information with other neurons nearby. The prolonged end of the axon is called the growth cone [101]. It consists of flat layers of cell membrane named lamellipodia from which extend filopodia that formed due to actin polymerization, and thanks to these structures the growth cone perceives the stimuli specific to the neural elongation in the environment and the axon structure begins to extend towards the main source of these stimuli. The growth cone then differentiates into the pre-synaptic neural terminal, developing synaptic vesicles containing neurotransmitter to interact with the dendritic structures of the subsequent cell. The synapse formation occurs due to the release of the neurotransmitters in the synaptic vesicles to the environment depending on the

action potential and the perception of the subsequent cell by the receptors in the dendrites. Neural cell binding molecules (N-CAM) on the axon binding surface, proteins such as cadherins (N-cadherin), fibronectin and laminin are known to affect elongation, migration, adhesion, and guidance [102].

These well-organized genetics program can inspire and inform techniques that can be utilized to take control of neuronal behavior in vitro, improving the topographic management and resolution of an engineered neuronal network.

Cell polarity is widely associated with the spatial differences in structure, shape, and function. In neural differentiation, symettery is broken and morphology changes to form dendrites and axons [103, 104]. Neurons are polarised, the information flows in one direction like dendritic synapes to cell body, and then to pre-synaptic terminal respectively. This flow is vital for nervous system function. For in vitro neuronal network obtaining convenient polarity is important. Functional polarity relies on anatomical property. Studies demonstrated that in development, axon-dendrite differentiation is started through both extracellular cues and intracellular signalling routes. Polarity is also observed in sub-cellular level, with organelles, protein complexes, and ion channels presented in different membrane areas or cellular elements [105].

For patterned in vitro neuronal networks, obtaining convenient polarity is remarkable challange. Differentiation neurons may have the ability to self-organise to form convenient polarity, but terminally differentiated cells may need certain topographic like guidance cues, or may be incapable to form convenient polarity.

1.4.4 Hydrogels to culture neurons

Hydrogels are a class of polymeric materials with physical and chemical specifications that make them helpful for cell growth. The platforms utilized for tissue development within synthetic regenerative environment needs scaffolding to supply an entire microstructure that mimics the ECM. Hydrogels provide 3D microstructure that is helpful for tissue regeneration and creates the primary basis for their utilization in neural regeneration. The simplicity and adaptability of hydrogels can be determined by their applicability in regenerating diversed tissue types like highly densed bone to

very soft tissues like liver, but they are especially appropriate for neural tissue regeneration [106].

Biophysical interactions within a hydrogel take place at the molecular scale, with solutes dissolved in aqueous state interacting with hydrated polymer chains at the lst order of organisation. Diffusion is a vital requirement to support cell functions in all ways for cellular system. Diffusion speed relies on the number and type of physical interactions that solutes meet when passing through the hydrogel. Denser and charged hydrogels can assist slower diffusion rates by enhancing the interaction of the matrix with solutes. This provides forming of gradients of factor and catch expressed factors close to cells. The chemistry of hydrogels also can be altered to assist the managed release of factors to utilize in drug delivery applications. Hydrogels have been utilized to manage the release of NGF, glial cell-derived neurotrophic factors, neurotrophin-3, insulin-like growth factor 1, brain-derived neurotrophic factor, epidermal growth factor, fibroblast growth factor, and vascular endothelial growth factor using the chemical conjugation, physical incorporation and drug saturated polymeric microspheres [107].

For the study of engineered neural systems, diversed hydrogel material have been examined (Figure 1.12). The cell in nervous system are attachment dependent so, the prepared culture matrices required to provide attachment sites for cell receptors. Cells also make connections with each other or with ECM that expressed or placed within the hydrogel. The quantity of ECM and other biological factors that absorbed or caught within hydrogel matrix influence the forming of cell niche. The reaction of ECM can be altered by hydrogel chemistry and by the speed and size of products that can diffuse through the hydrogel matrix. Cell morphology, regional search, and migration are altered by many hydrogel factors containing scaffold stiffness, porosity, and the presence of binding sites. Additionally, the forming of gradients or interruption of mechanical or biological characteristics within a hydrogel can be used to pattern cell behavior. Biological suitability, availability, cost, and changeability also determine material selection [107].

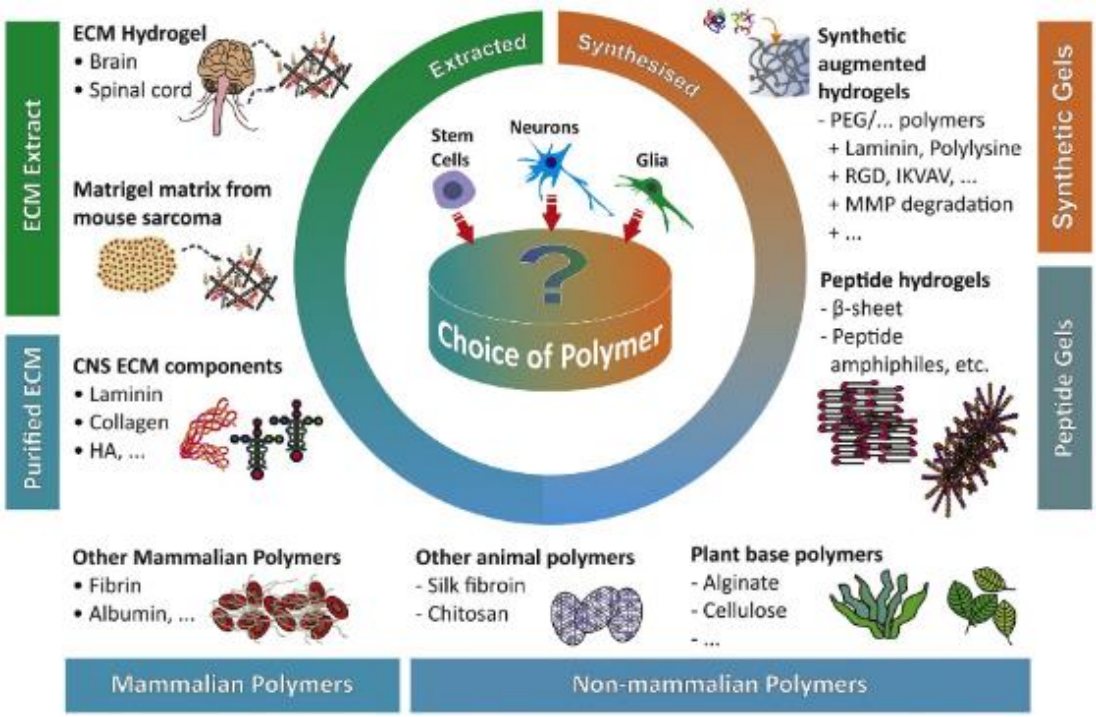

Figure 1.12. Different sources of polymer used in hydrogel preparations for nervous system studies [107].

Hydrogels have modifiable physical and chemical specifications, they are expected to compensate the requirements such as injectability, shear-thinning, self healing, biocompatibility, biodegradability, interactivity, porosity, and lack of swelling. They have great potential for future use in clinical applications of neuroregeneration. Hydrogel types primarily diversed as natural and synthetic hydrogels [108].

1.4.4.1 Natural hydrogels

Collagen is a key structural biopolymer that forms 30% of the mass of vertebrates and it is an ECM protein self-assembling into triple polypeptide helices. There are 28 proteins in humans named collagen and mostly known are collagen type I and type IV. Collagen type IV is broadly existed in the adult nervous system where it establishes basement membranes of the blood-brain barrier and neuromuscular junctions. Collagen type I assists axonal growth and guidance in neural development and in adults placed in the basal lamina of the subventricular zone. It is main part of connective tissue and supplies structure and support the body, containing skin, bones, cartilage, tendons, and nerves [108]. Brannvall *et al.* built up a two-component collagen type I-Hyaluronic acid (HA) (1:1 volume mix) matrix to improve the

differentiation of mouse embryonic, postnatal, and adult heterogeneous cell population of neural stem and progenitor cells [109]. The prepared network provided stability and suitable conditions for differentiation. The cells showed terminal differentiation with different signalling characteristics and showed synaptic links within the scaffold. Lee and friends studied the capabilities of laminin and fibronectin modified collagen to induce neuro-induction of rat bone marrow derived mesenchymal stem cells (BMSCs) in 2011 [110]. The prepared gel stimulated neural development of BMSCs without using chemical factors, probably thanks to low stiffness of the 3D collagen microenvironment. Hoban and collaborates presented proof for collagen type I as a non-cytotoxic and self-healing hydrogel in situ [111]. They injected the striatum of sham rats with glial cell line-reproduced neurotrophic factor trapped in a collagen with PEG ether tetrasuccinimidyl glutarate. The gel prohibited the micro and macrogliosis but, scaffold poorly supported mesenchymal stem cells survival and decreased in volume several days post gelation in vitro and in vivo.

HA is a glycosaminoglycan presented in extracellular tissues in diversed parts of the human body, and it has an important role in lubrication. HA has been successfully used broadly in neural tissue engineering due to the alterable specifications such as biodegradability, bioresorbability, biocompatibility, and hydrogel forming capability. In studies, it provides support for neurite outgrowth, differentiation, and proliferation on varied substrates, also improves the survival rates and proliferation of neural precursors [112]. Tian *et al.* implanted HA as a solid sponge to heal traumatic brain injury. HA wasn't successful alone but, when it modified with polylysine, neurons moved into hydrogel and created long neurites in vitro. Also when they implanted they were attended by astrocytes [113]. Wang and collaborates built a delivery system based on EDC (1-Ethyl-N,N-dimethylaminopropyl carbodiimide)-crosslinked HA that embedded brain-derived neurotrophic factor (BDNF) and vascular endothelial growth factor loaded poly(lactic-co-glycolic acid) (PLGA) microspheres. The prepared scaffold supplied steady release of VEGF and BDNF. It wasn't able to assist rat embryonic neural stem cells (NSCs) proliferation and survival [114].

Alginate is a naturally forming anionic biopolymer with forming a gel when bivalent cations like Ca^{2+} are added and mostly obtained from brown seaweed [112, 115]. It has great attract because of its low-cost, low-toxicity, biocompatibility and gelation

properties. However, its impurities like endotoxins, heavy metals, polyphenolic elements, and proteins are natural disadvantages because of its marine root. It has to be purified with multiple steps to minimize adverse impacts like inflammatory response [112]. Ashton and collaborates utilized alginate hydrogel to demonstrate enhancing the rate of degradation without harming rat neural progenitor cells (NPCs) [116]. They mixed alginate lyase-loaded PLGA microspheres into the hydrogel and saw that NPC proliferation was positively affected by rate of alginate degradation, and did not induce cell death. The control non-degradable hydrogel affected negatively the cell morphology and decreased the capability of NPCs to pass through the hydrogel. Suzuki *et al.* studied alginate at length in neural engineering. They demonstrated that alginate gels support peripheral nerve regeneration through a 50 mm long gap [117], in cat sciatic nerve and a 10 mm nerve gap in rats [118], increasing the diameter of the regenerating axons. They also used an alginate sponge for healing of facial nerves in cats. Repaired nerves in alginate indicated significant regeneration with 5 mm nerve defect size [119].

Chitosan is a structural polysaccharide reproduced by the chemical deacetylation of chitin, and presented in crab shell, and many sellfish. It has attractive characteristics such as gel creating abilities, high adsorption capacity, biodegradability, extremely biocompatible, tailorable, and presenting antibacterial activity. It has been highy used in neural engineering studies with showing cell adhesion, survival and interaction and neurite outgrowth [112, 115]. Cooper *et al.* produced an aligned chitosan-PCL (polycaprolactone) fibrous scaffold to examine its effect on cell adhesion, proliferation, and organization of Schwann cells (SC) and PC12 cells. The results showed that aligned PCL/chitosan fibers supported PC12 cell adhesion, and controlled the growth of cells along the fiber with showing improved unidirectional neurite extension and higher differentiation-specific gene expression [120]. Tseng and friends subjected zebrafish embryos to ethanol and later injected them either with phosphate-buffered saline (PBS), chitosan-based hydrogel, chitosan gel with scattered NSCs, chitosan with neurospheres, or cell suspension without gel [121]. The neuroprotective influences were studied via certain movements, natural contractions, and hatching of the embryos. Zebrafish with chitosan-neurosphere injection demonstrated enhanced functional recovery.

Fibrin is a fibirous natural enzymatically degradable protein presented in clotting of blood and lymph after injury. It is produced by the action of the protease thrombin on fibrinogen. It is highly biocompatible when it supplied from the autologous blood donor. Mooney and collaborates demonstrated that fibrin did not cause apoptosis and supported neuronal differentiation and growth of rat fetal NSCs [122]. All fibrin matrices with diverse stiffness that contolled by varying the ratios between the fibrinogen and thrombin, promoted an increase in cholinergic and dopaminergic neurons and blocked glial differentiation. Enhancing of stiffness supported growth of both dompaminergic neurons and glials. Itosaka and friends studied the fibrin matrix if it convenient scaffold in BMSC injection for the injured spinal cord of adult rats [123]. The results showed that fibrin matrix improves the survival, migration, and neural differentiation of BMSCs.

1.4.4.2 Synthetic hydrogels

Poly (α-hydroxy acid) polymers like poly(glycolic acid) (PGA) with, poly(lactic acid) (PLA), and their copolymers poly(lactic-co-glycolic acid) (PLGA) have been studied for diverse applications focusing on neural engineering. Both PGA and PLA are thermoplastic polymers, biodegradable and able to absorbed or hydrolyzed in vivo [112]. PLA was successfully utilized to design and built scaffolds mixing it with gelatin nanofiber that support Schwann cells for prolongation of axons, and vascular growth [124]. PGA-based nanoconduits showed great mechanical characteristics, but they gradually lose their strength after about 2 months upon implantation [125]. PLGA highly used in neural engineering due to its properties containing deformation, swelling, permeability, and alterable degradation rate. Xue *et al.* demonstrated that introducing autologous MSCs to a chitosan/PLGA scaffold enhanced the repair and rehabilitation of a 60 mm nerve gap after peripheral nerve injury in dogs [126].

Poly(ethylene glycol) (PEG) is a hydrophylic polymer which is a crucial property for nutrient and waste transport and attached only weakly to protein and cells. It is highly biocompatible and resitant to protein absorption and widely used. There are too many studies that showed neural cell growth on PEG platforms enhance cell survival, multiplication and, differentiation and has high potential for the treatment of CNS injuries [112]. Liu and friends demonstrated improved cell growth and migration along

with enhanced functional recovery in rats after transection of spinal cord using an electrospun PLGA/PEG scaffold [127]. Lampe *et al.* studied the effect of PEG macromere concentration on photo-encapsulated rat embryonic NPCs and found that astro-glial differentiation and glial-scar gene expression enhanced with increasing PEG content. Also higher PEG ingredient enhanced apoptosis and decreased metabolic activity in cells. PEG with 7.5% (wt) possessed similar stiffness with native brain and was the only hydrogel that assissted cell multiplication [128].

pHEMA (poly(2-hydroxyethyl methacrylate)) is another hydrophilic polymer that highly used neural engineering due to its tailorability to create similar mechanical characteristics with neural tissue. pHEMA can polymerise at low temperatures between -20ºC and +10ºC that lets immobilisation of proteins into hydrogels [112]. pHEMA firstly produced as porous hydrophilic sponge and provided a stable 3D scaffold able of assissting and supporting axonal regeneration in rats [129]. Soichet's group produced diverse pHEMA hydrogels able of guiding neurite outgrowth. By adjusting the formulation and surface chemistry, they are tailorable to suit in certain application in PNS or CNS. pHEMA hydrogel tubes successfully produced with similar mechanical specifications to spinal cord having 200 to 600 kPa elastic modulus [130].

1.5 Carbon Based Nanomaterials

Carbon-based nanomaterials offer unique electrical, mechanical, and biological properties that make them specifically suitable for tissue engineering. In too many studies for neural tissue engineering, graphene and carbon nanotubes were used for their natural properties of conductivity, flexibility, and biocompatibility.

Graphene is a 2D conductive nanomaterial that is formed by the perfect arrangement of a single layer of carbon atoms bonded with covalent bonds in a 2D hexagonal lattice like honeycomb. It greatly transmits electricity and heat. It is almost transparent, antiviral, bactericidal, and highly biocompatible with low cell toxicity. Graphene has been highly utilized for neural tissue engineering studies especially in the forms of foams and graphene nanogrids [112]. As 3D electrically conductive scaffold, the produced graphene foams induce and enhance differentiation and proliferation of

human neural stem cells [131, 132]. Graphene also has been utilized as material for neural probes, improving the quality of the neural-device interface [133].

Carbon nanotubes (CNTs) can be seen as derivaties of graphene, while graphene shows metallic behavior, rolling graphene sheets into CNTs forces periodic boundary conditions on the lattics, forming the possibility of a band gap. They have cylindrical structure qualified by spectacular thermal conductivity, optimal mechanical and electrical features. The range of CNTs varying from metals to semiconductors relying on the direction the graphene is rolled which defined as its chirality. Thus, its electrical features are chirality-dependent. CNTs can be produced from metal catalysts utilizing chemical vapor deposition, arc-discharge evaporation, or blasted from hunks utilizing high-energy pulses with a method called laser ablation. They have great potential for neural tissue engineering applications with their biocompatible, conductive, and non-biodegradable character. CNTs utilized as implants where long-term cues for neurite outgrowth are essential, like regeneration after brain or spinal cord injury. According to their structure, CNTs divided into two groups which are single-walled CNTs (SWCNTs) and multi-walled CNTs (MWCNTs) (Figure 1.13).

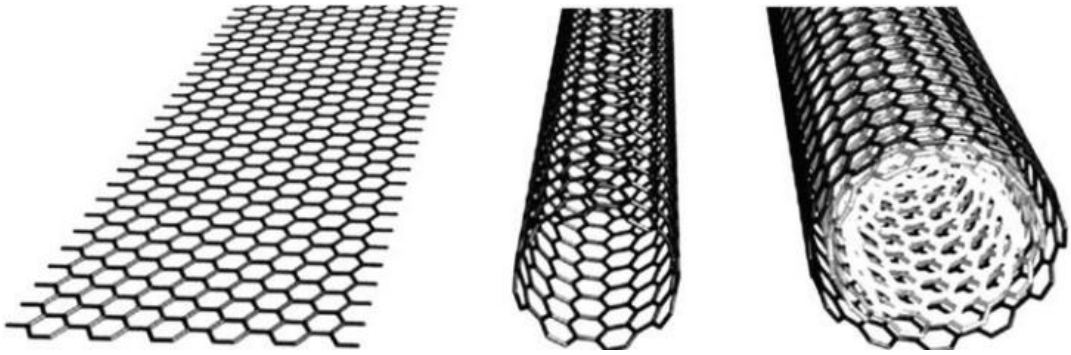

Figure 1.13. From left - graphene, SWCNT, MWCNT [134].

Geith and friends used SWCNTs as substrates that control and induce neural cells through the variations of conductance with using lateral currents for the aim of treating neurological and brain related injuries. MWCNTs utilized in novel technologies like 3D printing of scaffolds for peripheral nerve regeneration due to its high stability. CNT-hydrogel composites have been gained momentum with using multiple ways in which CNTs improving the hydrogels with great features such as enhancing the mechanical stability, gaining electroconductivity, and providing attachment sites for

cells or serving as drug delivery vehicles upon functionalization [135]. Imaninezhad *et al.* utilized polyacrylamide (PA) hydrogels and PEG-MWCNT nanocomposites with diverse stiffness and resistivity to test the synergistic influences of substrate stiffness, electro-conductivity, structure and electrical induction on the morphology, alignment, and directional neurite outgrowth using PC12 cells as model. Results showed that MWCNT added hydrogel substrate with combination of electrical induction provided enhanced conditions for neural growth and regeneration [136]. Shah and collaborates also developed MWCNT-PEG hydrogel to see its ability to support neural cell culture. They obtained that increase in CNT concentration resulted in increased gelation time, and decreased hydrogel stiffness. Also the hydrogel was suitable for PC12 cell culture providing higher cell viability with CNT ingredient compare to PEG hydrogel alone [137]. Shin and friends coated CNTs with a thin layer of gelatin methacrylate (GelMA) by utilizing the hydrophobic interactions between the polypeptide chains of GelMA and sidewalls of CNTs with allowing dispersion of CNTs in GelMA prepolymer. Addition of CNTs strengthened the GelMA hydrogels without decreasing their porosity or cell growth, and human MSCs readily spread and proliferated after encapsulation in CNT-GelMA hydrogel [138].

1.6 Dielectrophoresis

1.6.1 Theory of dielectrophoresis

Dielectrophoresis (DEP) was firstly developed in 1951 by Pohl as the translational movement of the dielectric, neutral particles caused by polarization effects in condition of non-uniform electric field [139]. Unlike electrophoresis where the particles moves through a viscous gel at a speed dependent on its charge and the applied DC electric field, in DEP, it does not need particles to be charged to manipulate with the electric field. The dipoles are stimulated by an AC electric field that causes movement at a speed dependent on relative polarizability [140]. DEP is divided in three groups based on interaction between the electric field and target matter including negative DEP (nDEP) where particles repelled from a region of high electric field strength, positive DEP (pDEP) where particles attracted to a region of high electric field strength, and combination of this two (Figure 1.14) [141].

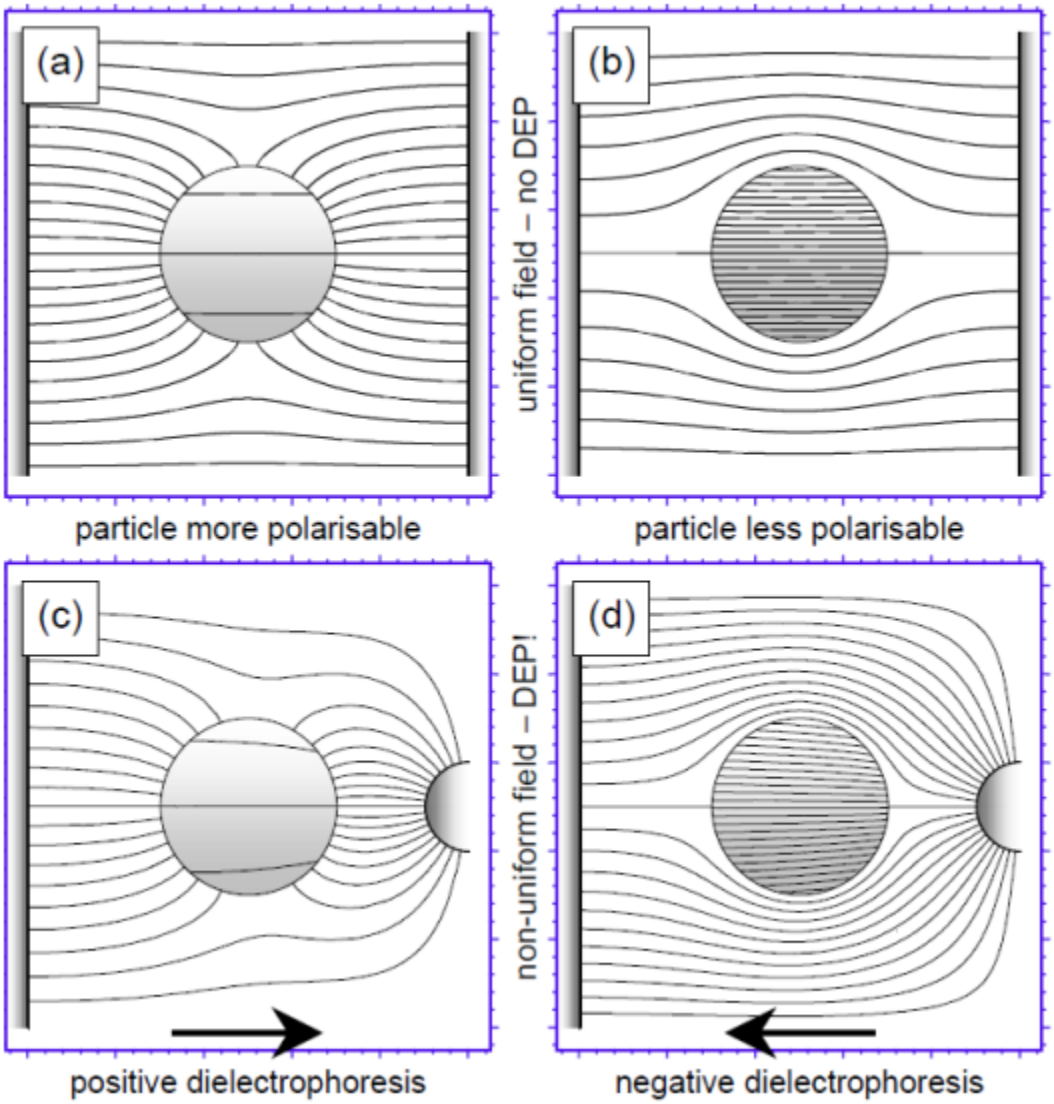

Figure 1.14. Electric field lines for four different situation depending on the polarizability of particle and medium; particle with higher (a) or less (b) polarizability than the medium in uniform electric field; particle being more (c) or less (d) polarizable than the medium in non-uniform electric field [142].

DEP has diverse aims in studies including separating, concentrating, or aligning the target matters. DEP can be also utilized to rotate or restrict the target matter like cells into desired locations as well as displacement [143]. Therefore, it has great potential as being versatile tool for controlling the cells in solution in microchip systems. In DEP, randomly oriented dipole in the electric field, so one end of the dipole exposes stronger electric field than the other causing non-zero net force which makes the dipole in motion. When the target particle is more polarizable than its surrounding medium,

the electric field lines bend against to the particle, but field strength is higher on one side of the particle than the other side resulting with imbalance of forces on the induced dipole causing in motion toward the strong field region with pDEP understanding. Conversely, when the particle is less polarizable than its surrounding medium, the particle demonstrates an opposite action by moving away from the strong field regions expressed as nDEP. Due to stimulated dipole is function of frequency, the polarizability of particle can be adjusted by performed frequency [144]. At low frequencies, the charges on the particle possess time to answer to the direction opportunity in the electric field with providing the particle more polarizability than the surrounding medium. Conversely, at high frequencies, the charges on the particle do not possess time to answer to the direction opportunity in the electric field with providing the particle less polarizability than the surrounding medium [145].

1.6.2 DEP based applications for cell patterning

There are many publications about the usage of the DEP technique in cellular applications which mainly are cell seperation, cell characterization, cell manipulation, and cell patterning [146]. DEP based 2D patterning techniques contains the utilization of 2D configuration of microelectrodes that creates an electric field gradient enough to affect and pattern cells near the surface in a single layer format of cell growth. Ho and friends fabricated a microfluidic chip to re-establish hepatic lobular structure utilizing p-DEP [147]. Titanium/platinum electrodes with concentric-stellate tip array were developed utilizing photolithography to pattern human hepatocellular carcinoma cells (HepG2) and human umbilical vein endothelial cells (HUVEC) cells. The cells were patterned in a low conductivity buffer with the parameters of 5 V_{pp} voltage and 1 MHz frequency and demonstrated high viability up to 95%. Hsiung *et al.* fabricated a microfluidic platform containing an array of planar interdigitated ring electrode (PIRE) using photolithography over indium tin oxide (ITO)-coated glass surface to utilize p-DEP [148]. They patterned HepG2 cells uniformly with about 50 cell per PIRE applying 5 V_{pp} voltage and 5 MHz frequency signal in EGTA-DEP buffer, the design of electrode let rapid and efficient patterning of the cells. In another study, an interdigitated electrode arrays using photolithograpy on ITO coated glass substrate containing four independent microelectrode subunits fabricated that placed on the top of the fluidic channel and cell patterning placed at the bottom of glass substrate with

utilizing of n-DEP [149]. The technique depended on patterning one type of cell with one electrode subunit to create one pattern and following with patterning another type of cell with another electrode subunit. They showed patterning of C2C12 cells with the parameters of 12 V_{pp} and 1 MHz into periodic and alternate line patterns and the device could be used in basic science to understand principle of cell to cell interactions. As alternative to chemical etching, a layer of insulating material such as SU-8 or polydimethylsiloxane (PDMS) had been utilized to perform nonuniform electric field for DEP-based manipulation and patterning. But, the studies showed that SU-8 and PDMS have fouling properties and do not provide long-term stability of described cell patterning. Tsutsie *et al.* utilized PEGDA polymer for addressing theses issues to create an array of micro-wells over ITO-coated glass which resulted with 95% cell viability and efficient and rapid patterning of mouse embryonic stem cells [150]. Şen *et al.* fabricated a DEP device with an array of 900 gourd-shaped microwell for pairing single cells of different types [151]. The design containing interdigitated array electrodes provided trapping of different cell types on opposite sides of the microwells. They applied pDEP to one of IDA combs with the parameters of 8 V_{pp} voltage and 1 MHz frequency AC signal to trap 3T3 cells in one side of the microwells. The same signal applied to another IDA comb to trap ES cells. Two types of cell were efficiently manipulated to create close pairs into desired locations with up to 80% success rates.

Because of the absence of suitability of cellular behavior and functionality with presence of insufficient cell to cell and cell to substrate interactions in 2D monolayer patterning techniques, the studies have also focused on the establishment of 3D cell patterning techniques. Mainly used methods includes collecting of cells in the form like 3D spheroid/microtissue, clustering with the 3D hydrogel, and alignment of cells in 3D spatial format with suitable electrode configurations that create a 3D electric field [152]. Yu and friends patterned neural cells in the form of 3D aggregate with n-DEP. Patterned neural cell clustes demonstrated good viability and created desired neuronal network on the bioelectronic chip itself [153]. Sebastian and collaborates optimized DEP parameters containing electrode size, applied voltage, and fluid speed on cellular aggregates [154]. They demonstrated the creating of AC3 and Jurkat cellular aggregates of 150 μm high using interdigitated oppositely castellated electrodes applying 20 V_{pp} and 1 MHz by p-DEP to study interactions between the

cells in 3D artificial micro-niches. Albrecht and friends utilized p-DEP to pattern 3T3 cells in PEGDA solution by photo-crosslinking of the PEGDA with the patterned cellular clusters with achieving high area cluster density with about 115 or 205 clusters per mm^2 of hydrogel relying on the array spacing with up to 90% viability for each cluster [155]. Neverthless, only 5-10 cells of clusters can be controled with changing DEP parameters and electrode dimesionality. Ramón-Azcón *et al.* demonstrated the patterning of myoblast (C2C12) and endothelial (HUVEC) in GelMA using DEP [142]. The study showed that GelMA based DEP provided better performance on patterning, migration, spreaded morphology, and long-term viability (more than 5 days) of the cell types, but in PEGDA hydrogels, cells had round morphology and demonstrated about 90% cell death at the fifth day of culture.

CNTs have gained remarkable interest in biological studies like cancer therapy, drug delivery, bioimaging, biosesensing, and tissue engineered scaffolding due to their unique mechanical, chemical, electrical, and optical features. Adding CNTs into tissue engineered scaffolds provides improved scaffold flexibility, strength, and electrical conductivity [156]. Using DEP to align CNTs in a hydrogel has been showed by Ramon Azcon et al [157]. They applied DEP with parameters of 20 V_{pp} voltage and 2 MHz frequency through an interdigitated array of Pt electrodes to align the MWCNTs in GelMA hydrogels and compared the mechanical and electrical properties of it with prisitine GelMA. The hydrogel was used to produce C2C12 muscle myofibers. Aligned MWCNTs enhanced electrical and mechanical features of the hydrogel resulting in myofibers with more maturation and contractility after electrical stimulation, and electrical stimulation also promoted muscle cell differentiation. Ahadian *et al.* utilized DEP to fabricate hybrid GelMA-aligned CNT gels and compared it against to pristine GelMA and GelMA with randomly dispersed CNT hydrogels [156]. DEP was utilized via interdigitated ITO electrode with parameters 20 V_{pp} voltage and 1 MHz frequency to horizontally align CNTs in the GelMA prepolymer. Hybrid hydrogel demonstrated superior efficiency in enhancing cardiac differentiation of mouse embryoid bodies in compared to control groups.

1.7 Scope of the Thesis

Worldwide there are millions of people experiencing some degree of nerve injury, mostly caused by traumatic events and diseases [136, 158]. Although neurons have some degree of capability to regenerate, functional recovery is mostly limited without a structural support. The local microenvironment has an important impact on the regulation of cell adhesion, differentiation, and proliferation. The establishment of functional nervous system requires guided neurite outgrowth, a process in which growing neurons produce connections via extensions [159, 160]. Tissue engineering offers promising approaches for designing scaffolds with suitable cues and properties for the development of neuronal circuits and induction of neuronal regeneration after injury [161, 162]. Developing in vitro models using tissue engineering techniques can be useful in a variety of ways, from understanding the regulatory mechanism of neurite outgrowth to identifying possible drugs which can reduce barriers to regenaration of nervous system [75]. Understanding the regulatory mechanism of neurite outgrowth is crucial not only in understanding brain development but also in finding new ways to induce neurite re-outgrowth in patients with neurodegenerative diseases [163].

The aim of the present study was to demonstrate the impact of randomly distributed MWCNTs in poly (ethylene glycol) dimethacrylate (PEGDMA) on PC12 cell differentiation in terms of neurite length, number of neurite per cell and differentiation marker gene expression profile, and to represent the guiding and supporting performance of PEGDMA with dielectrophoretically aligned MWCNTs on the neural differentiation of PC12 cells in the presence of NGF.

The results of the study showed that the represented platform had a great potential for guiding neural outgrowth and producing neuronal circuits for diverse applications ranging from nerve regeneration to drug discovery.

2. EXPERIMENTS

2.1 Materials

Collagen (type IV, 0.5-2 mg/ml) (Sigma-Aldrich, USA), acetic acid (Sigma-Aldrich, USA), poly-L-lysine (Sigma-Aldrich, USA), trypsin (Gibco, USA), donor horse serum (DHS) (Capricorn, Germany), fetal bovine serum (FBS) (Sigma-Aldrich, USA), L-glutamine (Gibco, USA), gentamicin (Gibco, USA), RPMI 1640 (Sigma-Aldrich, USA), nerve growth factor (NGF) (Vipera lebetina venom) (Sigma-Aldrich, USA), phosphate buffered saline (PBS) (Sigma-Aldrich, USA), multiwalled carbon nanotube (MWCNT) (Nanografi, Turkey), 98% H_2SO_4 (Sigma-Aldrich, USA), 68% HNO_3 (Sigma-Aldrich, USA), Irgacure (Sigma-Aldrich, USA), PEGDMA (PolyScience, USA), 3-(Trimethoxysilyl)propyl methacrylate (Sigma-Aldrich, USA), acetone (Sigma-Aldrich, USA), isopropyl alcohol (IPA) (Sigma-Aldrich, USA), ethanol (Sigma-Aldrich, USA), NaOH (Sigma-Aldrich, USA), AZ5214E reversal photoresist (MicroChemicals, Germany), AZ1505 (MicroChemicals, Germany), AZ400K developer (MicroChemicals, Germany), AZ 100 developer (MicroChemicals, Germany), calcein AM kit (Biotium, USA), DMSO (Sigma-Aldrich, USA), live/dead double staining kit (Dojindo, Japan), mRNA extraction kit (Wizbio, South Korea), cDNA synthesis kit (QuantaBio, USA), SYBR (Wizbio, South Korea), 200 nmol primer standard (Atlas Biyoteknoloji, Turkey).

- GAPDH (Forward primer: 5’-TGGCGCTGAGTACGTCGTG-3’; Reverse primer 5’-ATGGCATGGACTGTGGTCAT-3’),
- GAP43 (Forward primer: 5’; AGAAAGCAGCCAAGCTGAGGAGG-3’; Reverse primer: 5’-CAGGAGAGACAGGGTTCAGGTGG-3’),
- synapsin I (Forward primer: 5’-CAGGGTCAAGGCCGCCAGTC-3’; Reverse primer: 5’-CACATCCTGGCTGGGTTTCTG-3’)

2.2 PC12 Cell Culturing

For the initial part of the study, PC12 cells with neural networking capacity were used for culturing. Since the PC12 cells are semi-suspended cells due to their nature, surface coating was needed. To be sure about the best coating for cell attachment, some cells were grown on poly-L-lysine (PLL) coated surface and some of them were grown on collagen coated surfaces. All coating processes were completed in the cell culture cabinet to prevent any contamination and just in case, the coated flasks were UV sterilized before usage (Figure 2.1). The surface of the flasks were first coated with PLL. For PLL coating, 3 groups were prepared as undiluted, diluted 10 times, and diluted 20 times with PBS. For coating, 2.5 mL solution of each group was poured onto the three different flasks that have 25 cm^2 surface area and were left in the incubator for 5 min. After incubation, excess solutions in the flasks were drawn with a pipette. Then, the PLL coated flasks dried at room temperature and stored at +4 ºC for later use. For the collagen coating, collagen solution was prepared with adding 5 mL of PBS solution containing 0.25% acetic acid into 0.5 mg of commercially purchased collagen. The prepared solution was shaken until it homogenized at 2-8 ºC. Then, it was transferred to small eppendorf tubes and removed for storage at -20 ºC in order not to spoil the protein structure of the collagen by subjecting it to freeze and thaw processes again and again. For the coating process, the prepared solution was poured onto the flask surface with a pipette and the solution was pipetted and released few times to be ensured that the solution covered the surface. The flasks were then incubated for 2 hours to coat the surface with collagen. After incubation, the flasks ,which were observed to be completely dry, were stored at 4 ºC for later use.

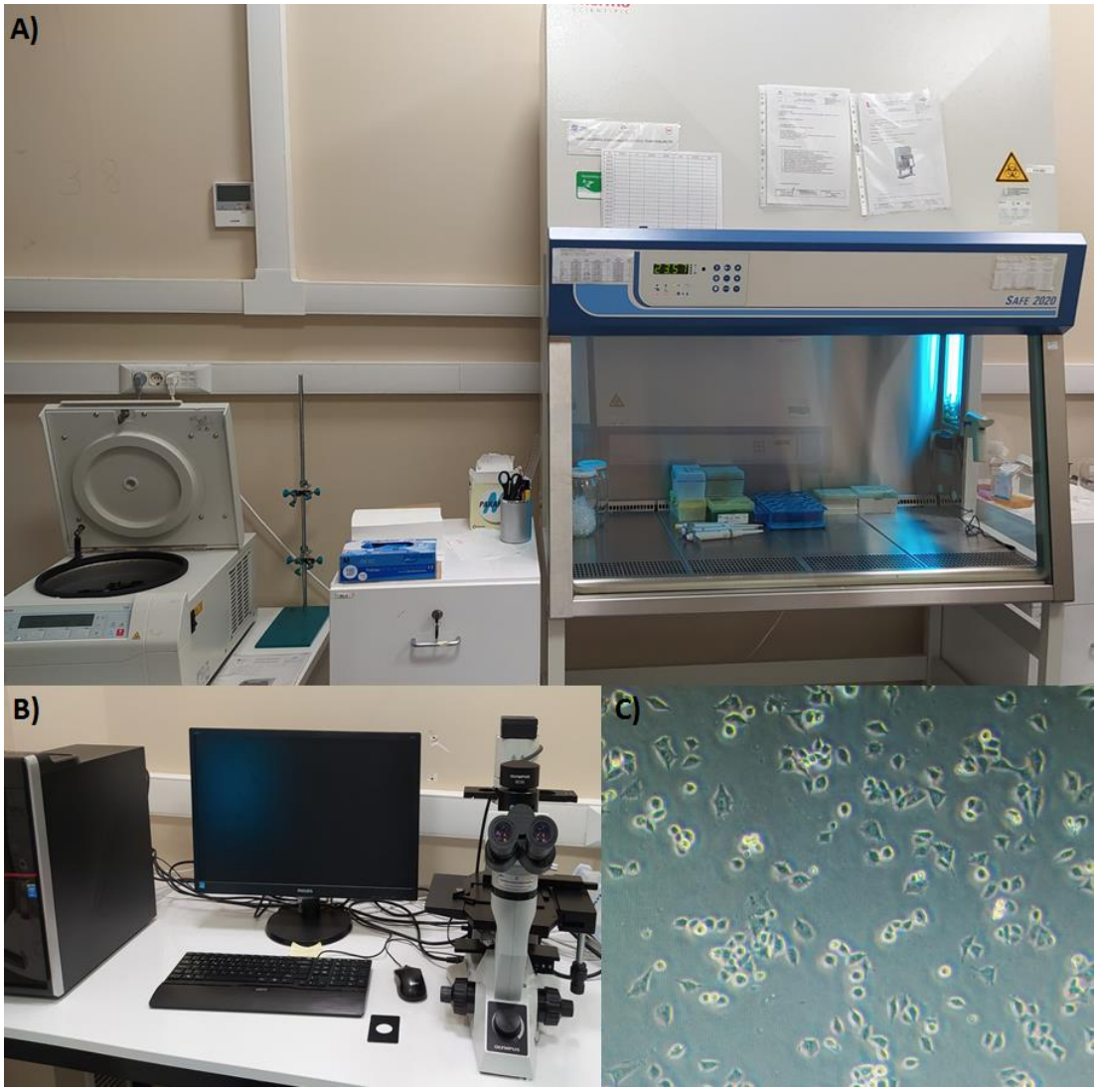

Figure 2.1. General view of the laboratory used for cell culture studies (A and B), and microscope image of cultured PC12 cells (C).

The purchased pre-frozen PC12 cells were thawed in the water bath until the half of them dissolved and they were centrifuged in a falcon tube at 1000 rpm at +4 ºC for 5 min, then, they were homogenized in 1 mL RPMI 1640 medium (containing 10% DHS, 1% FBS, 1% L-glutamine, and 0.1% gentamicin) with the help of vortex. This cell suspension was then transferred to cell culture flasks containing 4 mL of RPMI 1640 (10% DHS + 1% FBS + 1% L-glutamine + 0.1% gentamicin) medium. Subsequently, these flasks were placed in an incubator (EC160, Nüve, Turkey) at 37 °C and 5% CO_2, allowing the cells to grow in these flasks. When the flasks containing PC12 cells achieved a confluency between 80-90%, they were taken into the cell cabinet after the disinfection of the flasks with 70% ethanol to prepare them for the

passage. Firstly, the cells were washed with 5 mL PBS solution for about 30 sec in order to facilitate the removing of the cells from the surface. After washing, 1 mL of trypsin solution was poured in the flask and the flask was taken into the incubator for 5 min. Then, the flasks were checked under microscope to be sure that the cells removed from the surface. Next, the flask with lifted cells was taken back to the cell cabinet. 4 mL RPMI 1640 (10% DHS + 1% FBS + 1% L-glutamine + 0.1% gentamicin) medium was added to the flask containing lifted cells and trypsin solution, and the solution was transferred to the falcon tube. The falcon was centrifuged at +4 ºC, 1000 rpm for 5 min to precipitate the cells to obtain them cleanly. After the centrifugation process, the supernatant solution in the liquid form at the top was removed with the help of a pipette in order to use the collapsed cells at the bottom of the falcon. Then, the cells were suspended in 5 mL RPMI 1640 (10% DHS + 1% FBS + 1% L-glutamine + 0.1% gentamicin) medium, and 2 mL of suspension was transferred into the PLL coated and collagen coated flasks in 1 mL each for passaging in a ratio of 5:1, then the flasks were placed in incubator at 37 °C and 5% CO_2, allowing the cells to grow in these flasks.

During the passage process, the remained homogenized solution after the centrifuge were centrifuged again at 1000 rpm and +4 ºC for 5 min to precipitate the cells. When the cells were precipitated, the supernatant liquid above them were removed with pipette and freezing medium composed of 10% dimethyl sulfoxide (DMSO) and 90% FBS was added on the remained suspended cells. The solution was mixed via pipetting until it became homogenized and transferred into the freezing vials that is resistant to liquid nitrogen tank. Then, the freezing vials were placed to -80 ºC for transfering them to the liquid nitrogen tank after 2 weeks.

2.3 Effect of NGF on PC12 Cells

In the next stage of the study, the effects of commercially sold NGF on differentiation of PC12 cells were analyzed. Many studies in the literature have found that different methods and media combinations are preferred for the differentiation of PC12 cells. At this stage, different media combinations were also tested and the most suitable differentiation conditions were determined for the culturing of PC12 cells (Figure 2.2).

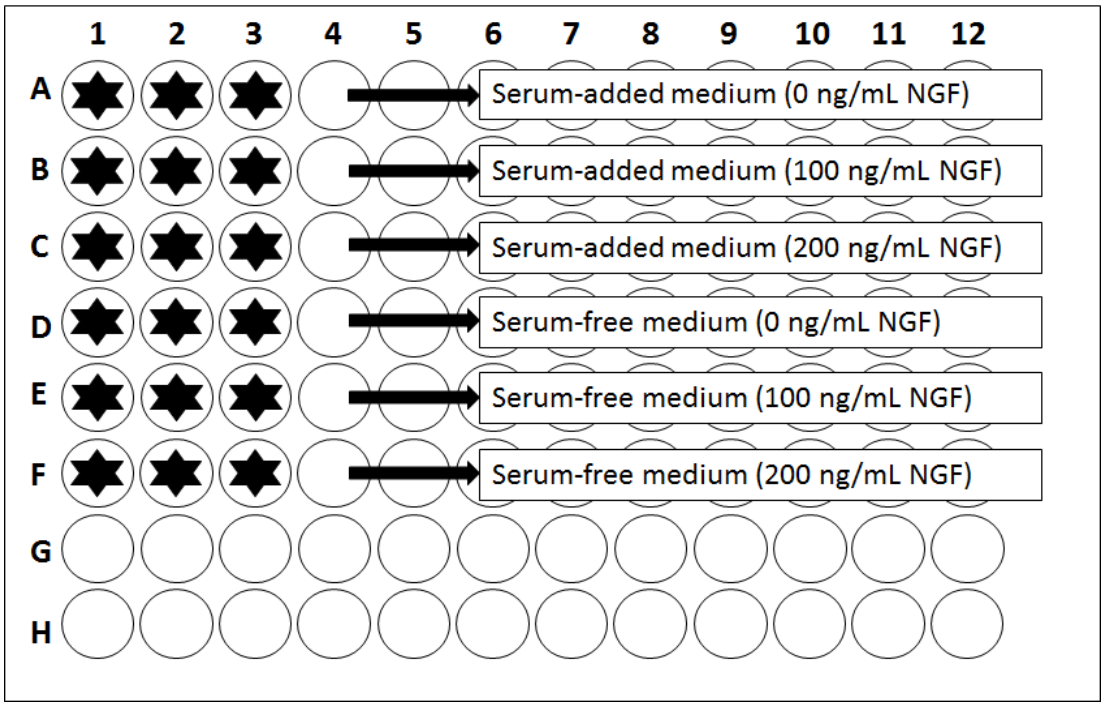

Figure 2.2. Experimental setup for the 6 different group of medium as serum-added and serum-free medium that combined with 3 different NGF concentrations (0,100,200 ng/mL) to examine the effect of medium content and NGF concentration on PC12 cell differentiation.

First of all, the purchased NGF was stocked for later use in the study. PBS containing 1 mg/mL protein was added to the NGF bottle in a sterile environment and the entire NGF contained in the bottle was dissolved in solution with the help of vortex. Since it was known that freezing and thawing processes could decrease the effectiveness of the enzyme, NGF solution was divided into small eppendorf tubes with a concentration of 500 ng/mL, each being 25 µL, and stored at -20 °C. The cells were cultured as described before. The passaged cells were added to the 96-well plate, which was previously coated with collagen, with $1x10^3$ cells per well. After cultivation of cells to the 96-well plates, they were incubated for 24 hours. In the next step, 6 different experimentral groups were prepared with two different medium as serum-added and serum-free medium that combined with 3 different NGF concentrations (0,100,200 ng/mL) and the cells were incubated in these medium groups for 6 days. Serum-added medium was containing the mixture of RPMI 1640 + 10% DHS + 1% FBS + 1% L-glutamine + 0.1% gentamicin, and the content of serum-free medium was including RPMI 1640 + 1% DHS + 1% L-glutamine + 0.1% gentamicin. Shortly, compare to

serum-added medium, the level of DHS was reduced from 10% to 1% and FBS was not added in serum-free medium. The medium of all groups was changed every 2 days for healthy differentiation of the cells. The cells were investigated under the microscope (CKX41, Olympus, Japan) everyday and their images were taken to understand the effect of NGF concentration in both serum-added and serum-free medium.

2.4 Preparation of PEGDMA and PEGDMA-MWCNTs Hydrogels

In this part of the study, previously commercially purchased MWCNTs were randomly dispersed in a biodegradable polymer called poly (ethylene glycol) (PEGDMA) and the effect of the prepared hydrogel on PC12 cell differentiation was investigated and compared with pristine PEGDMA. Firstly, 1% Irgacure was dissolved in ultrapure water using ultrasonic bath, then 10% PEGDMA was dissolved in this solution to prepare pristine PEGDMA prepolymer. Then, commercially purchased MWCNTs were precipitated by applying centrifuge for 30 minutes at 17000 rpm and in this way MWCNTs were washed three times with pure water to remove unwanted chemicals from the environment and reduce the conductivity. The washed MWCNTs were mixed with the prepolymer prepared in a homogenized manner and a PEGDMA prepolymer with a MWCNT concentration of 0.3 mg/mL was prepared. The prepared prepolymer mixture was polymerized in a chamber between 2 glass slides to provide a smooth surface for the cultivation of the cells in the next section. Firstly, one of the glass slides was washed with ultrapure water and treated with oxygen plasma to remove unwanted residues. The surface of the glass slide was then methacrylated with 3-(Trimethoxysilyl) propyl methacrylate (TMSPM) under vacuum for 1 hour. Surface modification was used to covalently attach the hydrogel to the glass slide, which was necessary to ensure that the cells can be cultured on the hydrogel for a long time without detachment. Then, 1 mm thick adhesive polyethylene terephthalate (PET) film spacer was placed between the surface modified and unmodified glass slides to form a chamber which was then filled with the PEGDMA-MWCNT prepolymer. The hybrid prepolymer was polymerized with UV light (7 mW/cm^2) for 3 min. After

polymerization, the surface modified glass-slide with hybrid hydrogel was detached and placed in a culture dish with the hydrogel on top. Also the pristine PEGDMA hydrogels were prepared in the same way and placed in culture dishes.

2.5 PC12 Cell Seeding on PEGDMA and PEGDMA with Randomly Distributed MWCNT Hydrogels

The entire surface of the both pristine PEGDMA and PEGDMA-MWCNTs hydrogels were coated with collagen (type IV, 0.5-2 mg/mL) to hold and spread the PC12 cell on the surface. PC12 cells were seeded on the hydrogels with a density of 5000 cells/cm^2 and cultured in RPMI 1640 medium supplemented with 10% DHS, 1% FBS, 1% L-glutamine and 0.1% gentamicin for 24 hours at 37 °C and 5% CO_2. The next day, the medium was replaced with a fresh medium containing 100 ng/mL NGF (Vipera lebetina venom) to induce cell differentiation. The medium with NGF was changed every 2 days. After 6 days culturing, the differentiation of PC12 cells were analyzed with regard to distribution of neurite length, number of neurites per cell and average neurite length.

2.6 Gene Expression

In this section, comparison of the cells grown above these 2 hydrogel groups were made according to the gene expression profile of 2 different gene markers named synapsin-1 and GAP-43. Synapsin-1 is required for synapse formation, whereas GAP-43 is considered a marker for axon re-generation. The expression levels of genes were normalized with respect to the internal reference gene GAPDH.

Real-time Polymerase Chain Reaction (Real Time PCR) method was used to numerically analyze the neural differentiation of 2 different groups of PC12 cells on pristine PEGDMA and PEGDMA with aligned MWCNTs hydrogels. In order for PCR to be performed, firstly the mRNAs of the cells must be removed, then they must be translated into cDNA for PCR. A kit was used to remove mRNA. First, the cells on the hydrogels were washed 1-2 times with PBS solution and trypsin was added to the cells for lifting. After waiting for 5 minutes in the incubator, PBS was added on the cell solution and suspended with a pipette, then the cells were collected from the

hydrogels and transferred to the eppendorf tubes. The cells were centrifuged at 13000 rpm for 5 min at room temperature. After centrifugation, the liquid was removed by pipette and the pellet of cells were remained. After adding 200 µL of RC buffer on the pellet and suspending it with a pipette, it was homogenized with the help of vortex and waited for 5 min to complete the chemical reaction. Then 300 µL of RL buffer was added to the solution. And 5 µL of 2-mercapto-ethanol was added onto it and mixed with the help of vortex then, waited for 5 min. Then, it was centrifuged with 13000 rpm at room temperature for 2 min. After centrifugation, the pellet part was remained, and 400 mL of the liquid was transferred to a new 1.5 mL eppendorf. After transferring to a new eppendorf, sterile 400 µL ethanol was added onto it and mixed via vortex. After placing the column with the tube, 800 µL solution was transferred into the tube column. It was centrifuged at 13000 rpm for 1 min at room temperature, then the column was removed from the tube. The tube was emptied and the column was put back into the tube. 500 µL of W1 solution was added to top. It was centrifuged at 13000 rpm for 1 minute at room temperature again, then the tube was separated from the column and the liquid was emptied from the tube. The same process was done with this time by adding 600 µL of W2 solution to the top and it was centrifuged at 13000 rpm for 1 min at room temperature, then the tube was separated from the column and the liquid was emptied from the tube. Next, W2 solution was added again and the process was repeated. Likewise, after separating the column with the tube and emptying the liquid from the tube, it was placed in the tube and centrifuged empty for 3 min at 13000 rpm without adding anything. After the centrifugation, the column and tube were separated from each other and the tube was removed, and the column was placed in the new eppendorf. There was a filter at the bottom of the column, 30 µL of RNA Prewater was added in the middle of the filter and it was waited for 3 min. Then, it was centrifuged at 13000 rpm for 3 min. The column was removed after centrifugation and mRNAs were collected in the eppendorf.

In order to convert to cDNA, firstly, the absorbance values of the mRNAs were examined via NanoDrop device, and accordingly the dilution ratio was found. According to the absorbance values, the best results were obtained with dilution ratio of 1:10. Then, the samples were taken into the cabinet to convert mRNAs to cDNA. During this process, the QuantaBio cDNA synthesis kit was used. 10 µL of free water,

4 µL mix, 1 µL RT solution, and 5 µL mRNA were added to the solution and all was mixed with the help of vortex and centrifuged for 10 seconds. Next, the centrifuged solution was placed in the PCR device, and kept at 22 ºC for 5 min, 42 ºC for 30 min, 85 ºC for 5 min and last at 4 ºC. Thanks to these processes, mRNAs were converted to cDNA.

For PCR processing, cDNAs were diluted in a ratio of 1:10 with autoclaved ultrapure water. At this stage, all the processes were carried out on ice. To prepare the mix, GapDH-F and GapDH-R were mixed via spinning and vortex. Then, 50 µL of the mix was taken and combined in an eppendorf. The process was repeated for forward (F) and reverse (R) genes for each gene. Then, to prepare a master mix, SYBR, ultrapure water, ROX and pre-prepared mix were prepared with separate solutions for each gene. Since the plate had 3 replicates, 15 µL of master mix solutions for each gene were added to 3 different wells, and 5 µL of 10 times diluted cDNA solution was added to each well. The plate was covered with a seal and the obtained cDNA was left for reading on a real-time qPCR device (Step One Plus Real-time PCR system, Applied BioSystems, USA) with appropriate gene-specific primers (GAPDH, synapsin-1 and GAP43). The forward and reverse primer sequences are as follows; GAPDH: 5'-TGGCGCTGAGTACGTCGTG-3'/5'-ATGGCATGGACTGTGGTCAT-3', GAP43: 5'-AGAAAGCAGCCAAGCTGAGGAGG-3'/5'-CAGGAGAGACAGGGTTCAGGTGG-3' and synapsin-1: 5'-CAGGGTCAAGGCCGCCAGTC-3'/5'-CACATCCTGGCTGGGTTTCTG-3'. The differential expression of the genes was quantified by StepOne Software v2.3 and normalized against that of the GAPDH gene. The gene expression analysis was repeated at least three times for each sample.

2.7 Fabrication of Au Interdigitated Array (IDA) Electrode

In this part, the fabrication of the microchip and the production of masks for photolithography, which will form the basis for the new platform developed. Vectorworks program was used for microchip design. The success of the MWCNT to be aligned with dielectrophoresis (DEP) depends on the electrical field to be created with the electrodes. Therefore, varied electrode designs were prepared for providing

alignment of MWCNTs as zigzag structures (Figure 2.3). Considering the effect of the electric field and the distance between the electrodes in the alignment of the CNTs, the distance between the electrodes was determined as 50-100 μm in order to achieve a successful result. It was thought that this distance will be sufficient for the extension of axon and dendritic structures. The design, which was output from the Vectorworks program in DXF format, was then converted to GDS format with the Layout program for the laser mask writing machine. 12.6 × 12.6 mm ready-made chrome mask was used in mask production. Chromium side was coated with AZ1505 positive photoresist using "spin coater". Later, the prepared designs were transferred onto the mask with Heidelberg brand (DWL 66FS) laser mask writing machine. In the next part, the areas that become sensitive as a result of laser application were removed with a solution of "AZ400K developer" mixed with pure water in a ratio of 1:4, and the chromium located in the areas where the photoresist was removed was etched with sodium nitrate/perchloric acid solution, also known as chrome "etching" solution. The photoresist that remained in unetched regions where was removed with "AZ 100 developer remover".

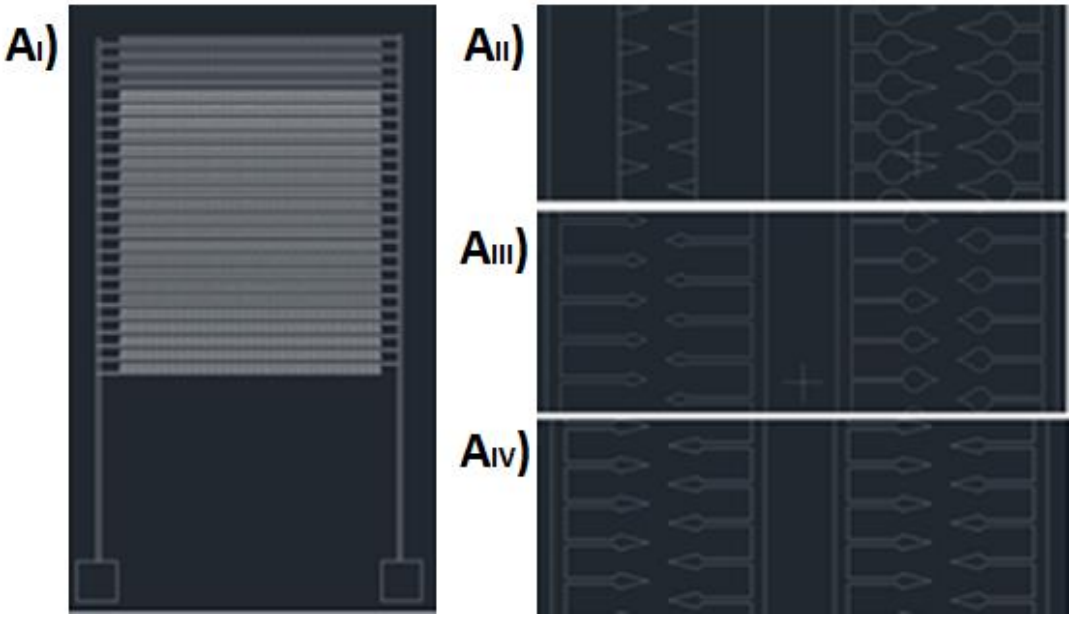

Figure 2.3. Mask design with four different shapes drawn with the Vectorworks program to ensure that the carbon nanotubes are aligned as zigzag (Ai, ii, iii-iv).

After the production of chrome masks, the fabrication of Au interdigitated array electrode (IDA) microchips was made in Izmir Institute of Technology Clean Room (Figure 2.4) with using photolithographic methods (Figure 2.5)

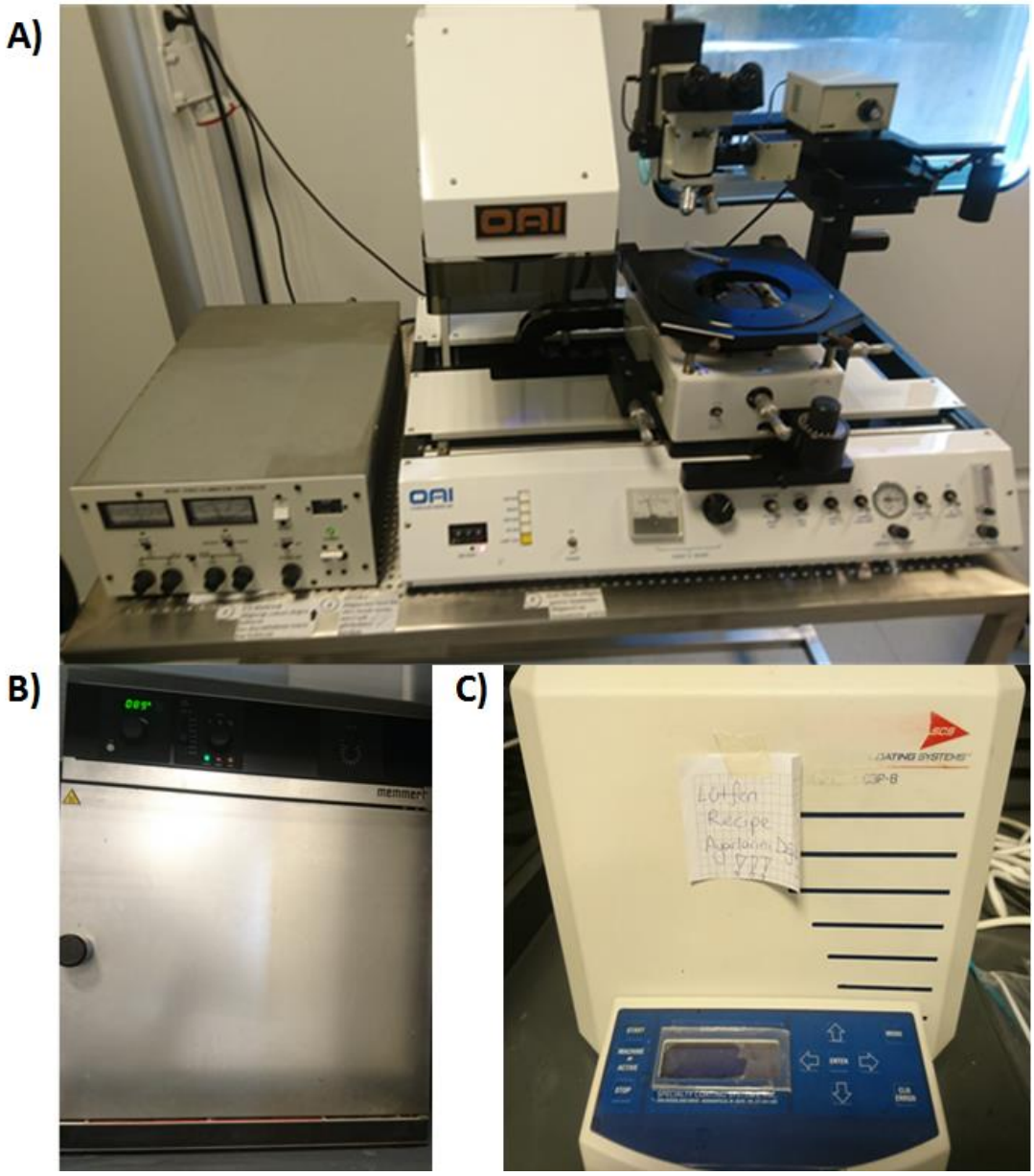

Figure 2.4. The devices that was used for microchip fabrication in Izmir Institute of Technology Clean Room: UV-mask aligner (A), oven (B), Spin-Coater (C).

Firstly, Au coated glass substrates (slide) were cleaned with various liquids (ultrapure water, acetone, isopropanol) with ultrasonic methods and treated with oxygen plasma to remove undesired residues. Then the surface of Au coated glass slides were coated with a positive/reversal photoresist AZ5214E via “Spin-Coater” at 2000 rpm for 60

sec. The polymerization of photoresist (pre-baking) was provided by keeping the photoresist-coated substrates in an oven set at 90 °C for 30 minutes.

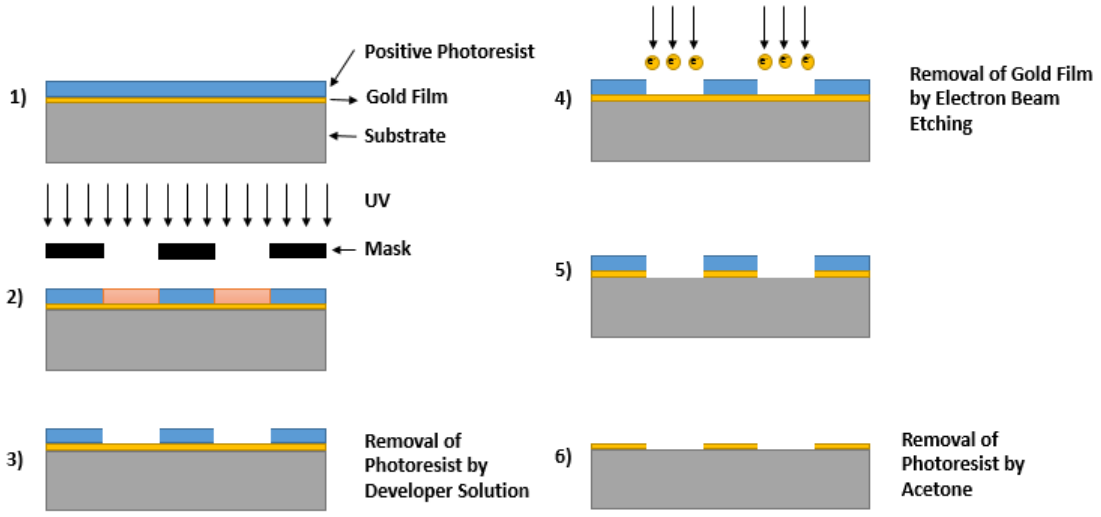

Figure 2.5. Fabrication steps of the Au-IDA microchip using photolithography.

In the following micro-fabrication step, patterning was carried out using chrome lithography mask produced specifically for the microchip. Before this process, the lithography mask to be used were first cleaned with the help of pure water and acetone, and dried with a special dust-repellent cloth and nitrogen gun. The cleaned and controlled lithography mask was placed in the UV mask aligner. The photoresist coated slide to be used was removed from the oven and cooled for a while, then fixed under the mask with the help of double-sided tape. The shapes on the mask were exposed to UV light for 16 seconds with the help of UV mask aligner and transferred onto photoresist coated slides. In order to remove the UV-exposed areas, a cheap and effective solvent (developer) was prepared using a mixture of 0.8 g NaOH and 100 mL distilled water. The slides were separated from the mask and placed in the developer, which was prepared in order to remove the areas that become sensitive after UV light exposure (positive photoresist basic understanding) by shaking gently for 7 sec, so that the necessary shapes for the microchip were passed on Au coated slides with the photoresist. Afterwards, slides were rinsed in distilled water and dried with the help of nitrogen gun. In the last step, the control of the dried slides was carried out under a microscope. The checked microchips that were taken to the ion beam etching device for etching. Firstly, the device was operated with “Rough Pump”, when the pressure

dropped to the mtorr level, and then, the pressure dropped to the µtorr level with the turbo molecular pump. After the vacuum has been activated, the necessary parameters for etching have been entered into the device. For Au-coated slides, etching was performed by rotating the sample holder at an angle of 22.5 degrees for 1 hour using parameters of 750 V, 49 W, 0.05 A with 30 sccm Argon gas. Since the photoresist coated part is resistant to this process, the parts where the photoresist was removed were abraded on Au-coated slides. After the microchips produced, they were checked under a microscope and with a multimeter to prevent possible short circuits. Finally, the photoresists on the remaining shapes were removed with acetone.

2.8 Preparation of Dielectrophoretically Alignment of MWCNT in PEGDMA Hydrogel on Au-IDA Microchip

In the next step, the alignment of the commercially purchased MWCNTs in PEGDMA with utilizing DEP technique was performed on the Au-IDA microchip to guide and support the neural differentiation of PC12 cells in the presence of NGF (Figure 2.6).

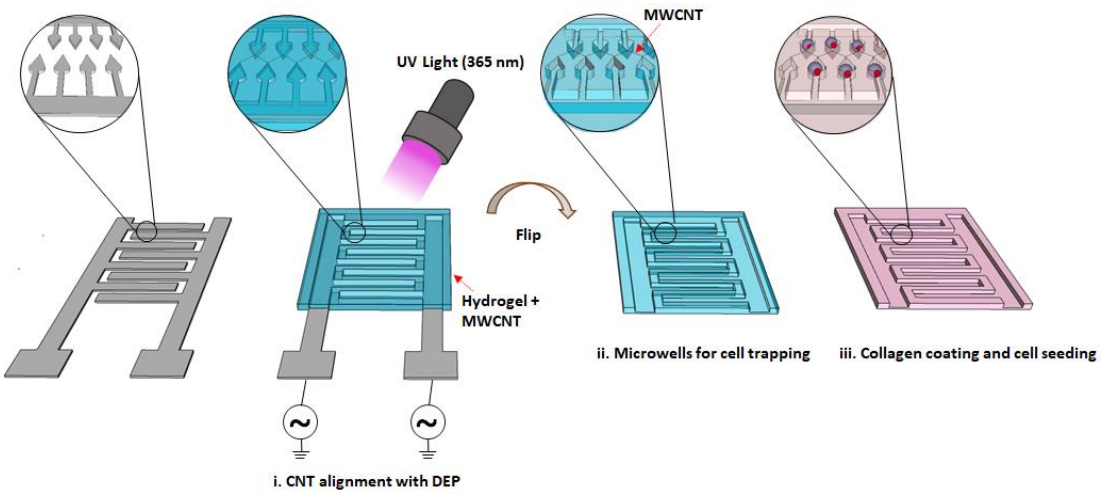

Figure 2.6. A schematic illustration of the strategy used to align and fix MWCNTs in PEGDMA. CNTs were aligned in PEGDMA on an IDA using DEP and then fixed via UV crosslinking. The gel with aligned CNTs was peeled off, flipped and placed in a culture dish. Following coating the whole surface with collagen, PC12 cells were seeded on the gel and cultured for 24 h at 37 °C. The next day, NGF was added to the medium to induce neuronal growth.

A 1 mm thick PET film spacer was placed between the TMSPM surface modified glass slide and the Au-IDA microchip that was prepared previously to form a channel for the previously prepared PEGDMA prepolymer with 0.3 mg/mL concentration of MWCNTs. To create non-uniform electric field for the alignment of MWCNTs, DEP was applied with the parameters of 10 Vpp sinusoidal AC voltage with the same frequency (1 MHz) and opposite phase through the two micro-bands of Au-IDA microchip using a waveform generator (33500B, Keysight, USA). After standing for 1 min, the PEGDMA prepolymer containing aligned MWCNTs was polymerized by exposure to UV light (7 mW / cm^2) for 3 min. After polymerization, the hybrid hydrogel was removed from the DEP device and the hydrogel was placed on top in a culture dish. Here, the hydrogel was covalently attached to the glass slide due to surface modification with TMSPM.

2.9 Electrical Properties of PEGDMA and Hybrid Hydrogels

Firstly, the current-voltage (I-V) curves of pristine PEGDMA, PEGDMA with randomly distributed MWCNTs and PEGDMA with dielectrophoretically aligned MWCNTs were obtained using the two-probes of a source / measure unit (B2902A, Keysight, ABD) connected to a computer. The measurement was performed in a Faraday cage at room temperature to decrease noise. The voltage was swept between -2 and 2 V at a scan rate of 0.1 V/s and the resulting current was recorded. The measurement was conducted using the connection pads of the IDA microchip. Next, electrochemical impedance spectroscopy (EIS) measurements were performed for the same test groups using an Autolab PGSTAT204 potentiostat (Metrohm, Netherlands). The data were monitored and analyzed using Autolab Nova software. Impedance spectra of all the samples were recorded on the Au-IDA microchips over a frequency range of 1 to 100 Hz with a 25 mV perturbation amplitude.

2.10 Contact Angle Measurements of PEGDMA and The Hybrid Hydrogels

Surfaces of pristine PEGDMA, and hybrid hydrogels were compared with water contact angle measurements based on hydrophilicity by KSV Attension Teta goniometer (Biolin Scientific, Sweden). Briefy, 10 μL deionized water was poured onto the surface of hydrogels, imaged and the contact angle (θ) was measured.

2.11 PC12 Cell Seeding on PEGDMA Containing Aligned MWCNTs

The entire surface of the hydrogels was covered with collagen (type IV, 0.5-2 mg/mL) for allowing the PC12 cells to hold and spread on the surface. PC12 cells were seeded on the hydrogel at a density of 2000 cells/cm^2 (Figure 2.6) and they were supplemented with RPMI 1640 medium containing 10% DHS, 1% FBS, 1% L-glutamine and 0.1% gentamicin to culture them for 24 hours in an incubator at 37 °C and 5% CO_2. The next day, the medium was replaced with a fresh medium containing 100 ng/mL NGF (Vipera lebetina venom) to induce cell differentiation. The cells were cultivated for 6 days, and the medium with NGF was changed every 2 days.

2.12 Cell Staining and Fluorescence Imaging

After the 6 days of cultivation, the cells on the PEGDMA with aligned MWCNTs hydrogel were prepared for cell staining to take images of them. “Live/dead double staining kit” was used for staining the cells for fluorescence imaging. The protocol included in the kit was applied for the staining procedure. Firstly, the cells on the hydrogels were washed 3 times with PBS solution. The washed cells were then incubated in 1 mL of Calcein-AM/EthD-1 solution containing 2 μL of calcein-AM and 4 μL of EthD-1 (ethidiumhomodimer-1) at 37 °C and 5% CO_2 for 60 min for allowing the cells to stain. After incubation, the stained cells were washed 3 times with PBS again. After the staining process, the cells were placed under fluorescent microscope (Axio Vert.A1, Zeiss, Germany) and their images were taken via microscope camera (AbCam, UK).

3. RESULTS AND DISCUSSIONS

3.1 Effect of NGF on PC12 Cells

In some studies in the literature, it has been reported that a better differentiation is seen when PC12 cells are cultured in the presence of NGF with medium containing low concentrations of serum. As a result of this study, it was observed that PC12 cells were unable to maintain their viability in serum-free medium, but it was also observed that some of the cells were differentiated in the presence of NGF. PC12 cells cultured on serum-added medium was proliferated as expected. In the both serum-added and serum-free medium without NGF, the presence of protrusions called neuritis from the cells, which is also a symptom of differentiation, was not found, while in the presence of NGF, the cells differentiated and long protrusions became evident. When NGF was used as 200 ng/mL, a slight differences compared to 100 ng/mL were observed, but considering the NGF stock, it was concluded that 100 ng/mL NGF could trigger differentiation at the desired size. In fact, in some places with 100 ng/mL NGF concentration, longer neurites were detected compared to the conditions containing 200 ng/mL NGF. When the differentiation levels of the cells were compared in the presence of NGF in both serum-added and serum-free medium, it was found that the cells were differentiated significantly better in the serum-added medium. As a result of these findings, in the next parts of the study, serum-added medium (RPMI 1640 + 10% DHS + 1% FBS + 1% L-glutamine + 0.1% gentamicin) was preferred with the concentration of 100 ng/mL NGF for the differentiation of PC12 cells.

3.2 Differentiation of PC12 Cells on both PEGDMA and PEGDMA-MWCNTs Hydrogels

First the differentiation behaviour of PC12 cells was investigated on randomly distributed MWCNTs in PEGDMA in comparison to PEGDMA hydrogel.

Briefly, the pristine hydrogel was prepared with dissolving 10% PEGDMA and 1% Irgacure in ultrapure water and it was mixed with pre-washed MWCNTs with the concentration of 0.3 mg/mL to obtain PEGDMA with randomly distribute MWCNTs. The cells were seeded and allowed to differentiate on a flat surface. To achieve that, the hydrogel was polymerized in a chamber between two glass slides. The prepared hydrogels were then treated with UV light for polymerization between 2 glass slides that one of them was modificated with TMSPM. The surface modification with TMSPM was used to covalently bind the hydrogel to the modified glass slide, which was necessary to culture cells on the hydrogel for a long time without detachment. Also a PET film spacer (thickness, 1 mm) was placed between the surface modified and an unmodified glass-slides to form a chamber and determine the thickness of the hydrogels. Finally the UV-polimerized hydrogels were detached and coated with collagen for PC12 cell seeding. The cells were cultured on the hydrogels for 6 days with changing the medium once every 2 days.

After 6 days of differentiation, PC12 cells were analyzed in terms of distribution of neurite length, number of neurites per cell and average neurite length. The optical images showed that PC12 cells differentiated better on MWCNT-PEGDMA hybrid hydrogels (Figure 3.1). The histogram of neurite length and number of neurite per cell (Figure 3.2 (Ai-ii)) clearly showed very different patterns for the two hydrogels. An average neurite length for each group was calculated by taking the longest 50 neurites into account and it was appeared that the average neurite length for PC12 cells grown on PEGDMA (108.23 ± 37.02 μm) was significantly lower than those grown on PEGDMA-MWCNTs (196.98 ± 31.83 μm) (Figure 3.2 (Aiii)).

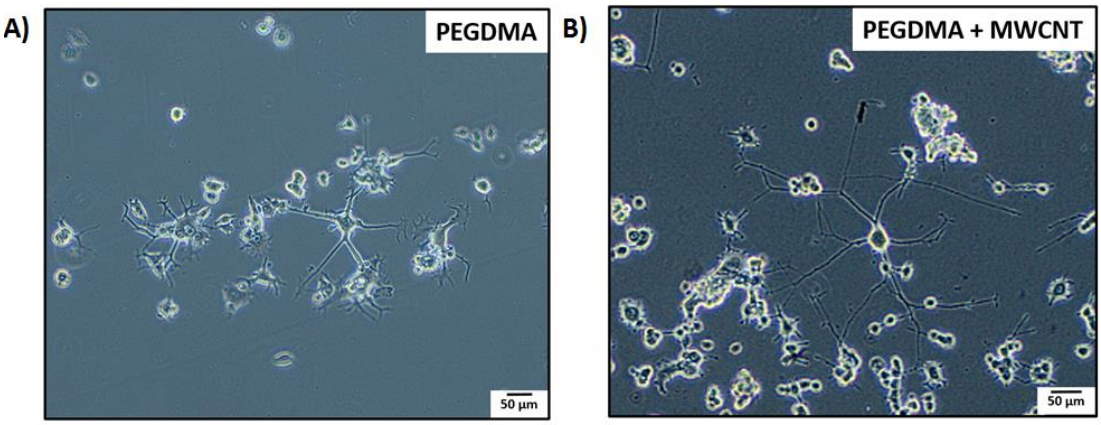

Figure 3.1. Optic images of PC12 cells cultured for 7 d on PEGDMA (A) and PEGDMA+MWCNT (random) (B), respectively.

These two hydrogels were also compared based on gene expression profile of two differentiation markers; synapsin-1 and GAP-43. Synapsin-1 is required for synapse formation, whereas GAP-43 is considered a marker for axon re-generation [164, 165]. The expression levels of genes were normalized with respect to the internal reference gene GAPDH. Figure 3.2 (B) clearly showed that the expression of the two markers increased significantly on the hybrid hydrogel as compared to PEGDMA in the presence of NGF. Altogether, the results clearly showed that PEGDMA+MWCNTs presented a better surface and microenvironment for the differentiation of PC12 cells. In other words, CNTs had a profound effect on neurite outgrowth by providing nanotopographical cues.

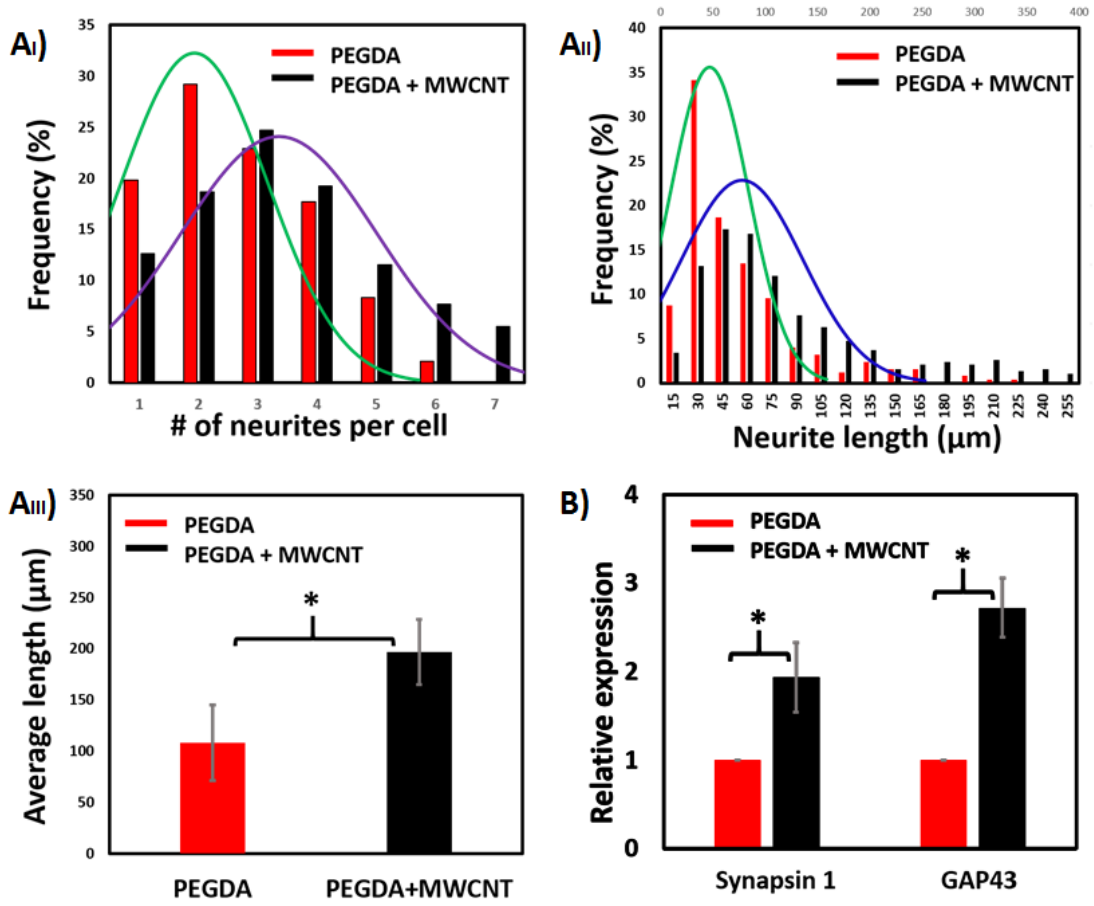

Figure 3.2. Analysis of the cells in terms of distribution of neurite length (Ai), number of neurites per cell (Aii) and average neurite length (Aiii). The expression of neuronal markers synapsin 1 and GAP-43 was also performed at day 7 using real-time PCR (B) (* $p < 0.05$).

3.3 Fabrication of Au Interdigitated Array (IDA) Electrode

A lithography mask was designed for the fabrication of the Au-IDA microchip. In the design, the electrodes were shaped in triangles and crenellated to ensure that MWCNTs were aligned in a zig-zag shape. The mask was used to fabricate an Au-IDA on a glass slide by conventional photolithography [166]. The Au in the UV exposed areas of the chip was removed with electron beam etching. After photolithography, "ion-beam etching" was preferred. Because the photoresist/metal film removal process known as "lift-off" is relatively difficult and has a low chance of success for Au coatings.

On the microscope images of microchips containing some different shapes that designed to provide the alignments of MWCNTs as zigzag structures, the distances between 2 electrodes were varied between as 93.5 μm and 114.9 μm (Figure 3.3).

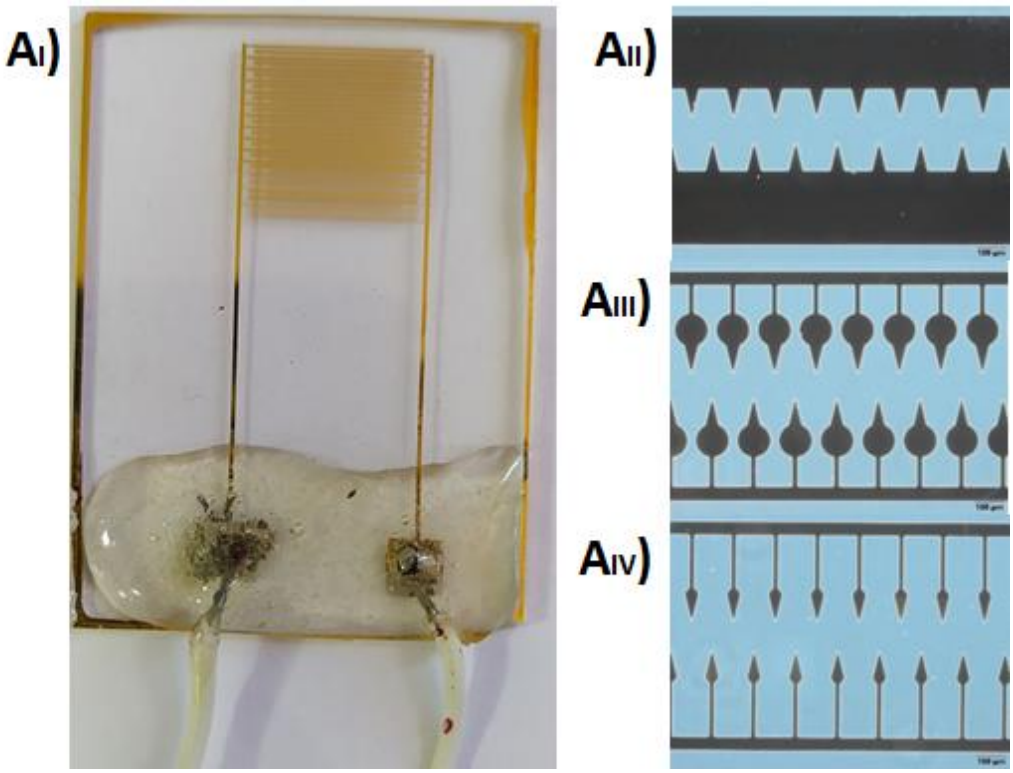

Figure 3.3. Au IDA microchip (Ai) and close-up images of microchip containing some shapes that will allow carbon nanotubes to be aligned as zigzag (Aii-iii-iv).

The measured electrode distances were very close to the values specified in the mask design, which shows the success of fabrication process.

3.4 Electrical Properties of PEGDMA and Hybrid Hydrogels

The fabricated Au-IDA microchip was used to align and fix MWCNTs in PEGDMA [167, 151]. Same as before, a PET film spacer (thickness, 1 mm) was used to create a chamber between the microchip and the TMSPM surface modified glass-slide. After filling the chamber with PEGDMA + MWCNTs prepolymer, the MWCNTs were aligned using DEP with applying a sinusoidal AC voltage of 10 V_{pp} with identical frequency (1 MHz) and opposite phase to the two microband arrays of the Au-IDA

microchip using a waveform generator (33500B, Keysight, USA) to create a nonuniform electric field for the alignment the CNTs, and fixed via UV polymerization of the hydrogel. Prior to cell experiment, the DC conductivity of PEGDMA with aligned CNTs was obtained using a source / measure unit and compared to those of pristine PEGDMA and PEGDMA with randomly distributed MWCNTs. The measurement was conducted using the IDA microchip before removing the hydrogel from the chip. As can be seen in Figure 3.4 (A), aligned MWCNT tracks drastically enhanced the conductivity of PEGDMA. A similar trend was observed in impedance analysis which was obtained in frequency range of 1 to 100 Hz with a 25 mV perturbation amplitude (Figure 3.4 (B)).

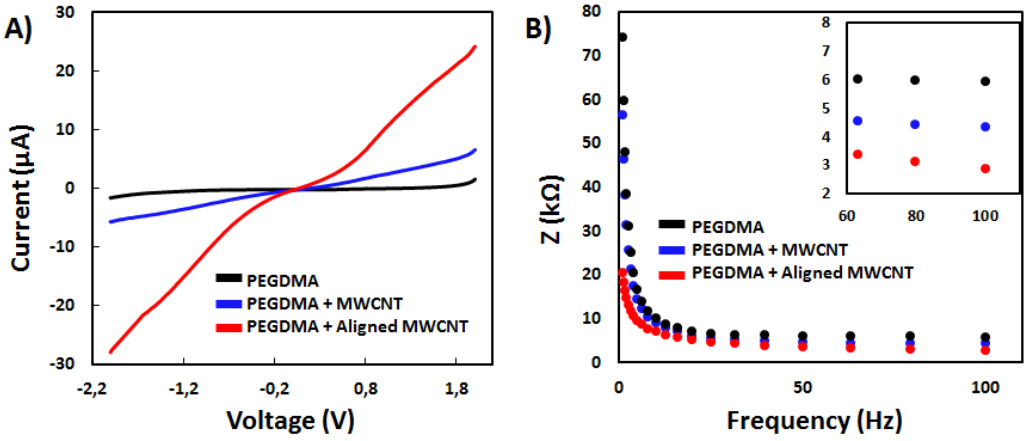

Figure 3.4. I-V curves (A) and impedance measurement results (B) of PEGDMA with no, random and aligned CNTs.

3.5 Contact Angle Measurements of PEGDMA and The Hybrid Hydrogels

Surfaces of pristine PEGDMA, and hybrid hydrogels on hydrophilicity was demonstrated using water contact angle (θ) measurement. The water contact angles were calculated depended on the photograph taken right after 10 µL of deionized water was dropped to the pristine PEGDMA surface and it was compared with the surfaces of hybrid hydrogels (Figure 3.5).

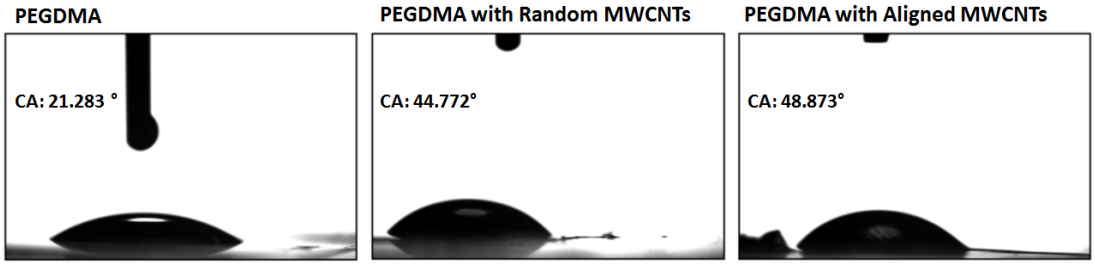

Figure 3.5. Measurement of water contact angle of the pristine PEGDMA, PEGDMA with random MWCNTs, and PEGDMA with aligned MWCNTs.

It can be easily seen in Figure 3.5 that the contact angle (θ) increased from 21.283 up to, 44.772º, and 48.873º for pristine PEGDMA, PEGDMA with random MWCNTs, and PEGDMA with aligned MWCNTs, respectively. MWCNT content provided hydrophobicity for PEGDMA surface, therefore covering the surfaces of the hybrid hydrogels with collagen provided better cell attachment.

3.6 Behaviour of PC12 Cells on PEGDMA Containing Aligned MWCNTs Hydrogel

Next, the hybrid hydrogel with aligned MWCNTs was detached from the DEP device for the cell experiment and placed in a culture dish with the hydrogel on top. Here, the hydrogel became covalently linked to the glass slide due to the surface modification with TMSPM. After collagen coating as before, PC12 cells were seeded on the gel with a cell density of 2000 cells/cm^2. The cells were allowed to attach the surface for 24 h. An AFM analysis showed that the Au electrodes had a thickness around 0.39 μm (Figure 3.6). Since, the micropatterns were transferred to the hybrid hydrogel after UV irradiation, it was assumed that the micropatterns in the hydrogels had a similar thickness which somehow mitigated the placement of PC12 cells close to aligned CNT tracks as shown in Figure 3.7.

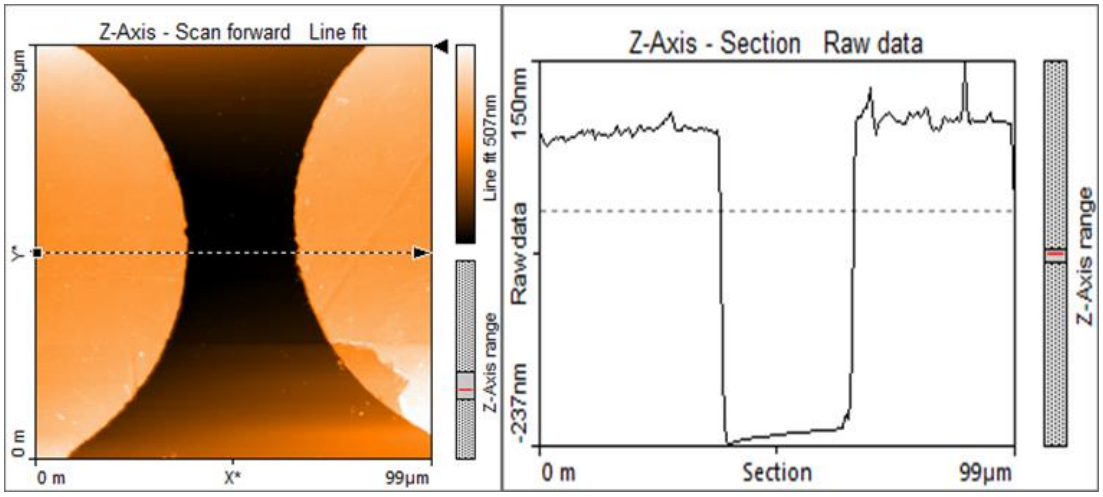

Figure 3.6. AFM was used to determine the height of electrodes and thus the depth of micropatterns in PEGDMA hydrogel.

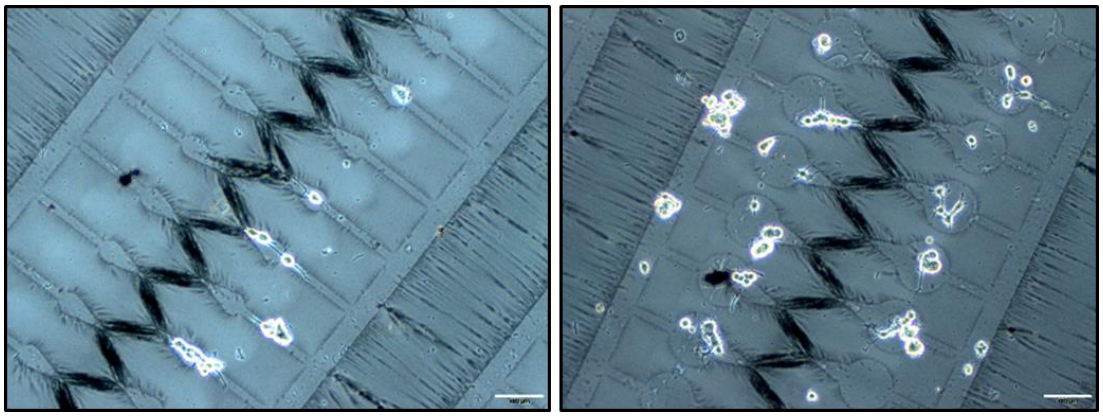

Figure 3.7. The micropatterns helped in entrapping cells and keep them close to aligned MWCNTs (CNT tracks).

The next day, differentiation medium was added and changed every 2 days. PC12 cells were allowed to differentiate for 6 days prior to imaging. Since the aligned CNTs were not transparent, the calcein AM dye was used to stain and thus, image the extensions of PC12 cells on these tracks (Figure 3.8 (Ai-iii)). Calcein AM is a dye that can pass through the cell membrane in most eukaryotic cells and can be used to determine cell viability. In the living cells, non-fluorescent calcein AM is converted into a green fluorescent calcein after acetoxymethyl ester hydrolysis with intracellular esterases. Aligned CNTs mediated the guidance of neural extensions (Figure 3.8 (Ai)) and connecting PC12 cells (Figure 3.8 (Aii)). Figure 3.8 (Aii) clearly shows that MWCNT tracks had a good performance in directing the neural outgrowth as extensions of both cells grew in two directions along the CNT tracks. In Figure 3.8 (Aiii), the extension

of a neuron had an approximately 37° deflection from the original trajectory when the extension reached a CNT track in which case the CNT track successfully directed the extension of the neuron to a different path.

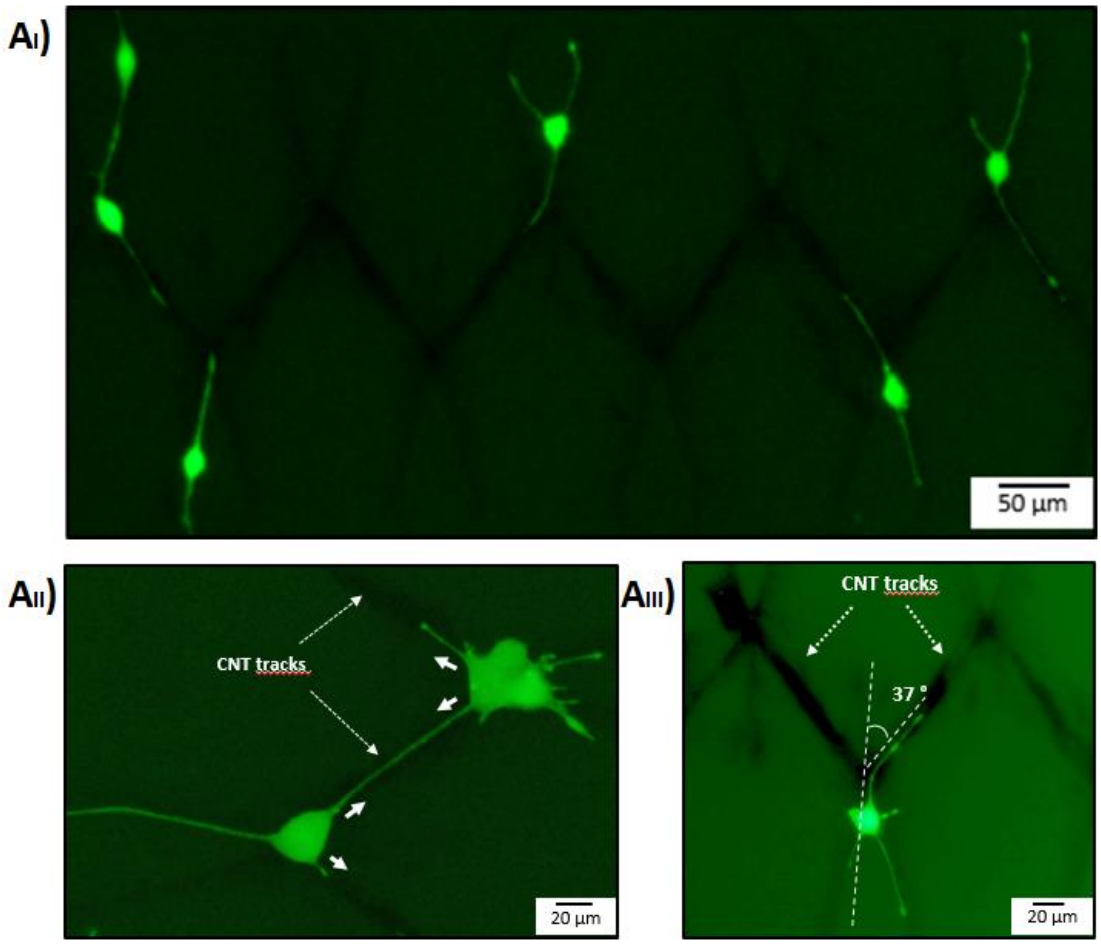

Figure 3.8. The MWCNT tracks mediated the guidance of neural extensions (Ai) and connecting PC12 cells (Aii). A clear deflection in neural extension can be observed when the extension reached the MWCNT tracks (Aiii).

In addition, cells that have both at least one visible neural extension and in contact with CNT tracks (n = 156) were analyzed to demonstrate the performance of CNT tracks in directing neurites (Figure 3.9). According to the results, 87.82 % of the cells had at least one neural extension guided by the CNT tracks; 59.62 % of the cells had one and 28.20 % of the cells had two neural extensions guided by the CNT tracks. 12.18 % of the cells had at least one neural extension but no apparent one guided by the CNT tracks.

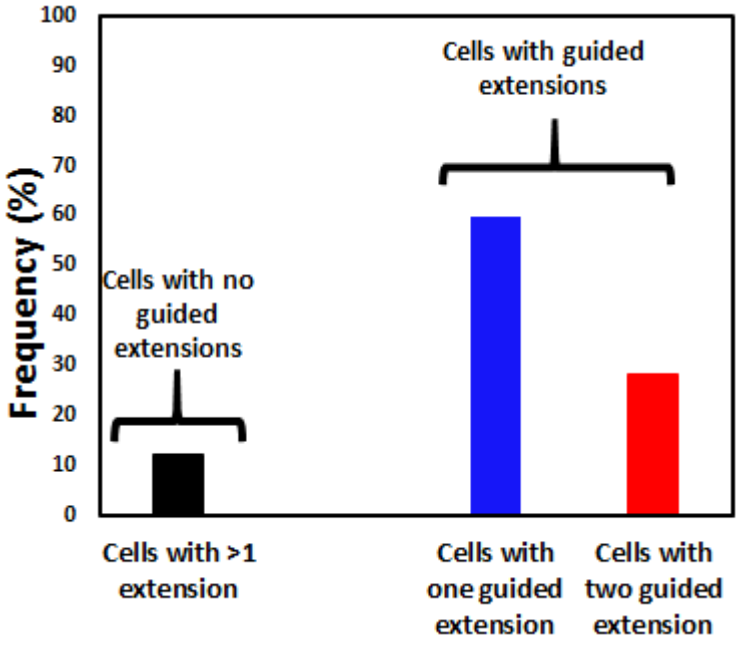

Figure 3.9. Frequency of cells with extensions guided by the MWCNT tracks.

There are various reports emphasizing the profound effect of nanotopographical features on controlling the directional growth and polarity [168]. It can be used to control cell fate in regenerative medicine. Basically, path-finding behaviour and neural outgrowth of neurons are governed by filopodia and lamellipodia and the dynamic stability of the two determines the response to nanotopographical cues.[169] Here, many single CNTs were brought together by dielectric force to form the CNTs. These tracks basically provided instructive physical cues for the two actin-based molecular structures to recognize and to subsequently modify their cytoskeletal structure, which resulted in guidance of the neural outgrowth of PC12 cells.

4.CONCLUSIONS

In this study, it was aimed to demonstrate the effect of randomly distributed MWCNTs in PEGDMA on PC12 cell differentiation in terms of neurite length, number of neurite per cell and differentiation marker gene expression profile, and to show the guiding and supporting performance of PEGDMA with dielectrophoretically aligned MWCNTs on the neural differentiation of PC12 cells in the presence of NGF.

As concluded in this study, PC12 cells differentiated remarkably better on PEGDMA with randomly distributed MWCNTs than PEGDMA alone with higher average neurite length, higher number of neurite per cell and higher gene expression levels. This situation can be attributed to nanotopographical cues and higher conductivity that was provided by the MWCNTs. The contact angle measurements showed that addition of MWCNTs to PEGDMA enhanced the hydrophobicity of the hydrogel. Since collagen is hydrophobic in nature, enhancing hydrogel hydrophobicity may have helped providing a better surface for collagen coating and PC12 cell attachment. A microenvironment consisting of micropatterns and CNT tracks was created using an Au-IDA microchip in conjuction with DEP. The new microenvironment allowed roughly positioning of PC12 cells and guidance of neural extensions through the CNT tracks. The present method could be useful for revealing the nanotopographical role in fundamental studies. The represented platform has a great potential for guiding neural outgrowth and producing neural circuits for diverse applications ranging from nerve regeneration to drug discovery. It could also contribute to understanding of nanotopographical effects for biomedical applications where nerve regeneration from a position to a predefined direction is required.

REFERENCES

1. Snyder J, Hagan C, Bolon B, Keene C. 20—Nervous System. Comparative Anatomy Histology. 2018:403-44.
2. Ballios B, Baumann M, Cooke M, Shoichet M. Chapter 55—Central nervous system. Principles of Regenerative Medicine. 2011:1023-46.
3. Tuladhar A, Mitrousis N, Führmann T, Shoichet MS. Central Nervous System. Translational Regenerative Medicine: Elsevier; 2015. p. 415-35.
4. Kandel ER, Schwartz JH, Jessell TM, Biochemistry Do, Jessell MBT, Siegelbaum S, et al. Principles of neural science: McGraw-hill New York; 2000.
5. Reception S. Human Vision: Structure and function of the Human Eye-vol. 27. Encyclopaedia Britannica. 1987:179.
6. Amini R, Rocha-Martins M, Norden C. Neuronal migration and lamination in the vertebrate retina. Frontiers in neuroscience. 2018;11:742.
7. Jimbo. *The Nervous System*. Available from: https://climatereview.net/ChewTheFat/?p=1015 [Accessed 20th June 2020].
8. Hagan CE, Bolon B, Keene CD. Nervous system. Comparative Anatomy and Histology: Elsevier; 2012. p. 339-94.
9. Kumar N, Kumar R. Nanotechnology and Nanomaterials in the Treatment of Life-threatening Diseases: William Andrew; 2013.
10. Edition TE. Anatomy and Physiology Volume 2 of 3: Lulu. com; 2014.
11. Equity T. College Biology Volume 3 of 3: Lulu. com; 2014.
12. Cajal SR. Histology of the nervous system of man and vertebrates. History of Neuroscience. 1995(6).
13. Kreutzberg GW. Microglia: a sensor for pathological events in the CNS. Trends in neurosciences. 1996;19(8):312-8.
14. Baumann N, Pham-Dinh D. Biology of oligodendrocyte and myelin in the mammalian central nervous system. Physiological reviews. 2001;81(2):871-927.
15. Spassky N, Merkle FT, Flames N, Tramontin AD, García-Verdugo JM, Alvarez-Buylla A. Adult ependymal cells are postmitotic and are derived from radial glial cells during embryogenesis. Journal of Neuroscience. 2005;25(1):10-8.
16. Sierra A, Tremblay M-È, Wake H. Never-resting microglia: physiological roles in the healthy brain and pathological implications. Frontiers in cellular neuroscience. 2014;8:240.
17. Jessen KR, Mirsky R. The origin and development of glial cells in peripheral nerves. Nature Reviews Neuroscience. 2005;6(9):671-82.
18. Ohara PT, Vit J-P, Bhargava A, Jasmin L. Evidence for a role of connexin 43 in trigeminal pain using RNA interference in vivo. Journal of neurophysiology. 2008;100(6):3064-73.
19. Review ADNP. *Central Nervous System*. Available from: https://www.austincc.edu/apreview/PhysText/CNS.html [Accessed 20th June 2020].
20. Korhonen L, Putkonen N, Lindholm D. Proteasome Role in Neurodegeneration. 2009.
21. Skovronsky DM, Lee VM-Y, Trojanowski JQ. Neurodegenerative diseases: new concepts of pathogenesis and their therapeutic implications. Annu Rev Pathol Mech Dis. 2006;1:151-70.

22. Siuly S, Zhang Y. Medical big data: neurological diseases diagnosis through medical data analysis. Data Science Engineering. 2016;1(2):54-64.
23. Brookmeyer R, Gray S, Kawas C. Projections of Alzheimer's disease in the United States and the public health impact of delaying disease onset. American journal of public health. 1998;88(9):1337-42.
24. Samii A, Nutt, J. G., Ransom, B. R. Parkinson's disease. The Lancet. 2004;363(9423):1783-93.
25. Sardoiwala MN, Kaundal B, Choudhury SR. Development of Engineered Nanoparticles Expediting Diagnostic and Therapeutic Applications Across Blood–Brain Barrier. Handbook of Nanomaterials for Industrial Applications: Elsevier; 2018. p. 696-709.
26. Lindsay J, Laurin D, Verreault R, Hébert R, Helliwell B, Hill GB, et al. Risk factors for Alzheimer's disease: a prospective analysis from the Canadian Study of Health and Aging. American journal of epidemiology. 2002;156(5):445-53.
27. Gepshtein S, Li X, Snider J, Plank M, Lee D, Poizner H. Dopamine function and the efficiency of human movement. Journal of cognitive neuroscience. 2014;26(3):645-57.
28. Berganzo K, Tijero B, Gonzalez-Eizaguirre A, Somme J, Lezcano E, Gabilondo I, et al. Motor and non-motor symptoms of Parkinson's disease and their impact on quality of life and on different clinical subgroups. Neurología. 2016;31(9):585-91.
29. Shulman JM, De Jager PL. Evidence for a common pathway linking neurodegenerative diseases. Nature genetics. 2009;41(12):1261-2.
30. Seddon H. Three types of nerve injury. Brain, Behavior and Evolution. 1943;66(4):237-88.
31. Campbell WW. Evaluation and management of peripheral nerve injury. Clinical neurophysiology. 2008;119(9):1951-65.
32.Zayed R, editor MR Neurography: an emerging modality in the evaluation of the lumbosacral plexus and sciatic lesions2019: European Congress of Radiology 2019.
33. Feigin VL, Abajobir AA, Abate KH, Abd-Allah F, Abdulle AM, Abera SF, et al. Global, regional, and national burden of neurological disorders during 1990–2015: a systematic analysis for the Global Burden of Disease Study 2015. The Lancet Neurology. 2017;16(11):877-97.
34. Gooch CL, Pracht E, Borenstein AR. The burden of neurological disease in the United States: a summary report and call to action. Annals of neurology. 2017;81(4):479-84.
35. Friess H, Zhu Z-W, Di Mola FF, Kulli C, Graber HU, Andren-Sandberg Å, et al. Nerve growth factor and its high-affinity receptor in chronic pancreatitis. Annals of surgery. 1999;230(5):615.
36. Aloe L. Rita Levi-Montalcini: the discovery of nerve growth factor and modern neurobiology. Trends in cell Biology. 2004;14(7):395-9.
37. Levi-Montalcini R. Growth control of nerve cells by a protein factor and its antiserum. Science. 1964;143(3602):105-10.
38. Levi-Montalcini R, Booker B. Excessive growth of the sympathetic ganglia evoked by a protein isolated from mouse salivary glands. Proceedings of the National Academy of Sciences of the United States of America. 1960;46(3):373.
39. Cohen S. Purification of a nerve-growth promoting protein from the mouse salivary gland and its neuro-cytotoxic antiserum. Proceedings of the National Academy of Sciences of the United States of America. 1960;46(3):302.

40. Lambiase A, Micera A, Sgrulletta R, Bonini S, Bonini S. Nerve growth factor and the immune system: old and new concepts in the cross-talk between immune and resident cells during pathophysiological conditions. Current opinion in allergy clinical immunology. 2004;4(5):425-30.
41. Micera A, Puxeddu I, Aloe L, Levi-Schaffer F. New insights on the involvement of Nerve Growth Factor in allergic inflammation and fibrosis. Cytokine growth factor reviews. 2003;14(5):369-74.
42. Lambiase A, Rama P, Bonini S, Caprioglio G, Aloe L. Topical treatment with nerve growth factor for corneal neurotrophic ulcers. New England Journal of Medicine. 1998;338(17):1174-80.
43. Aloe L, Tirassa P, Lambiase A. The topical application of nerve growth factor as a pharmacological tool for human corneal and skin ulcers. Pharmacological research. 2008;57(4):253-8.
44. Landi F, Aloe L, Russo A, Cesari M, Onder G, Bonini S, et al. Topical treatment of pressure ulcers with nerve growth factor: a randomized clinical trial. Annals of internal medicine. 2003;139(8):635-41.
45. Matsuda H, Koyama H, Sato H, Sawada J, Itakura A, Tanaka A, et al. Role of nerve growth factor in cutaneous wound healing: accelerating effects in normal and healing-impaired diabetic mice. The Journal of experimental medicine. 1998;187(3):297-306.
46. Micera A, Vigneti E, Pickholtz D, Reich R, Pappo O, Bonini S, et al. Nerve growth factor displays stimulatory effects on human skin and lung fibroblasts, demonstrating a direct role for this factor in tissue repair. Proceedings of the National Academy of Sciences of the United States of America. 2001;98(11):6162-7.
47. Lambiase A, Coassin M, Sposato V, Micera A, Sacchetti M, Bonini S, et al. NGF topical application in patients with corneal ulcer does not generate circulating NGF antibodies. Pharmacological research. 2007;56(1):65-9.
48. Aloe L, Luisa Rocco M, Omar Balzamino B, Micera A. Nerve growth factor: a focus on neuroscience and therapy. Current neuropharmacology. 2015;13(3):294-303.
49. Lindsay RM, Harmar AJ. Nerve growth factor regulates expression of neuropeptide genes in adult sensory neurons. Nature. 1989;337(6205):362-4.
50. Verge V, Richardson P, Wiesenfeld-Hallin Z, Hokfelt T. Differential influence of nerve growth factor on neuropeptide expression in vivo: a novel role in peptide suppression in adult sensory neurons. Journal of Neuroscience. 1995;15(3):2081-96.
51. Otten U, Schwab M, Gagnon C, Thoenen H. Selective induction of tyrosine hydroxylase and dopamine β-hydroxylase by nerve growth factor: comparison between adrenal medulla and sympathetic ganglia of adult and newborn rats. Brain research. 1977;133(2):291-303.
52. Connor B, Dragunow M. The role of neuronal growth factors in neurodegenerative disorders of the human brain. Brain Research Reviews. 1998;27(1):1-39.
53. McAllister A. Neurotrophins and neuronal differentiation in the central nervous system. Cellular Molecular Life Sciences. 2001;58(8):1054-60.
54. Bäckman C, Rose GM, Hoffer BJ, Henry MA, Bartus RT, Friden P, et al. Systemic administration of a nerve growth factor conjugate reverses age-related cognitive dysfunction and prevents cholinergic neuron atrophy. Journal of Neuroscience. 1996;16(17):5437-42.
55. Dreyfus CF. Effects of nerve growth factor on cholinergic brain neurons. Trends in pharmacological sciences. 1989;10(4):145-9.

56. Jönhagen ME, Nordberg A, Amberla K, Bäckman L, Ebendal T, Meyerson B, et al. Intracerebroventricular infusion of nerve growth factor in three patients with Alzheimer's disease. Dementia geriatric cognitive disorders. 1998;9(5):246-57.
57. Tuszynski MH, Thal L, Pay M, Salmon DP, Bakay R, Patel P, et al. A phase 1 clinical trial of nerve growth factor gene therapy for Alzheimer disease. Nature medicine. 2005;11(5):551-5.
58. Granholm A-C, Albeck D, Bäckman C, Curtis M, Ebendal T, Friden P, et al. A non-invasive system for delivering neural growth factors across the blood-brain barrier: a review. Reviews in the Neurosciences. 1998;9(1):31-56.
59. Illum L. Transport of drugs from the nasal cavity to the central nervous system. European journal of pharmaceutical sciences. 2000;11(1):1-18.
60. Thorne RG, Emory CR, Ala TA, Frey II WH. Quantitative analysis of the olfactory pathway for drug delivery to the brain. Brain research. 1995;692(1-2):278-82.
61. Chen X-Q, Fawcett JR, Rahman Y-E, Ala TA, Frey I, William H. Delivery of nerve growth factor to the brain via the olfactory pathway. Journal of Alzheimer's Disease. 1998;1(1):35-44.
62. Malkoc V, Gallego-Perez D, Nelson T, Lannutti JJ, Hansford DJ. Controlled neuronal cell patterning and guided neurite growth on micropatterned nanofiber platforms. Journal of Micromechanics Microengineering. 2015;25(12):125001.
63. Bhatia S, Balis U, Yarmush M, Toner M. Microfabrication of hepatocyte/fibroblast co-cultures: Role of homotypic cell interactions. Biotechnology progress. 1998;14(3):378-87.
64. Chen CS, Mrksich M, Huang S, Whitesides GM, Ingber DE. Geometric control of cell life and death. Science. 1997;276(5317):1425-8.
65. Folch A, Toner M. Cellular micropatterns on biocompatible materials. Biotechnology progress. 1998;14(3):388-92.
66. Tempelman LA, King KD, Anderson GP, Ligler FS. Quantitating staphylococcal enterotoxin B in diverse media using a portable fiber-optic biosensor. Analytical biochemistry. 1996;233(1):50-7.
67. Paddle BM. Biosensors for chemical and biological agents of defence interest. Biosensors Bioelectronics. 1996;11(11):1079-113.
68. Pancrazio JJ, Whelan J, Borkholder DA, Ma W, Stenger DA. Development and application of cell-based biosensors. Annals of biomedical engineering. 1999;27(6):697-711.
69. Boland T, Xu T, Damon B, Cui X. Application of inkjet printing to tissue engineering. Biotechnology Journal: Healthcare Nutrition Technology. 2006;1(9):910-7.
70. Roth EA, Xu T, Das M, Gregory C, Hickman JJ, Boland T. Inkjet printing for high-throughput cell patterning. Biomaterials. 2004;25(17):3707-15.
71. Sanjana NE, Fuller SB. A fast flexible ink-jet printing method for patterning dissociated neurons in culture. Journal of neuroscience methods. 2004;136(2):151-63.
72. Smith RK, Lewis PA, Weiss PS. Patterning self-assembled monolayers. Progress in surface science. 2004;75(1-2):1-68.
73. Tu C, Huang B, Zhou J, Liang Y, Tian J, Ji L, et al. A microfluidic chip for cell patterning utilizing paired microwells and protein patterns. Micromachines. 2017;8(1):1.

74. Csucs G, Michel R, Lussi JW, Textor M, Danuser G. Microcontact printing of novel co-polymers in combination with proteins for cell-biological applications. Biomaterials. 2003;24(10):1713-20.
75. Belkaid W, Thostrup P, Yam PT, Juzwik CA, Ruthazer ES, Dhaunchak AS, et al. Cellular response to micropatterned growth promoting and inhibitory substrates. BMC biotechnology. 2013;13(1):86.
76. Zeck G, Fromherz P. Noninvasive neuroelectronic interfacing with synaptically connected snail neurons immobilized on a semiconductor chip. Proceedings of the National Academy of Sciences. 2001;98(18):10457-62.
77. Xie C, Hanson L, Xie W, Lin Z, Cui B, Cui Y. Noninvasive neuron pinning with nanopillar arrays. Nano letters. 2010;10(10):4020-4.
78. Dowell-Mesfin N, Abdul-Karim M, Turner A, Schanz S, Craighead H, Roysam B, et al. Topographically modified surfaces affect orientation and growth of hippocampal neurons. Journal of neural engineering. 2004;1(2):78.
79. Gabay T, Ben-David M, Kalifa I, Sorkin R, Ze'ev RA, Ben-Jacob E, et al. Electro-chemical and biological properties of carbon nanotube based multi-electrode arrays. Nanotechnology. 2007;18(3):035201.
80. Sorkin R, Greenbaum A, David-Pur M, Anava S, Ayali A, Ben-Jacob E, et al. Process entanglement as a neuronal anchorage mechanism to rough surfaces. Nanotechnology. 2008;20(1):015101.
81. Hubenthal F. Noble metal nanoparticles: synthesis and optical properties. 2011.
82. Subramani K, Ahmed W. Fabrication of peg hydrogel micropatterns by soft-photolithography and peg hydrogel as guided bone regeneration membrane in dental implantology. Emerging Nanotechnologies in Dentistry: Elsevier; 2012. p. 171-87.
83. Liu M, Ji Z, Shang L. Top-down fabrication of nanostructures. Nanotechnology. 2010;8.
84. Scotchford CA, Ball M, Winkelmann M, Vörös J, Csucs C, Brunette D, et al. Chemically patterned, metal-oxide-based surfaces produced by photolithographic techniques for studying protein-and cell-interactions. II: Protein adsorption and early cell interactions. Biomaterials. 2003;24(7):1147-58.
85. Tan W, Desai TA. Microfluidic patterning of cells in extracellular matrix biopolymers: effects of channel size, cell type, and matrix composition on pattern integrity. Tissue engineering. 2003;9(2):255-67.
86. Morin F, Nishimura N, Griscom L, LePioufle B, Fujita H, Takamura Y, et al. Constraining the connectivity of neuronal networks cultured on microelectrode arrays with microfluidic techniques: a step towards neuron-based functional chips. Biosensors and bioelectronics. 2006;21(7):1093-100.
87. Kim DH, Kim PSS, Lee K, Kim J, Kim MJ. Galvanotactic behavior of Tetrahymena pyriformis under electric fields. Journal of Micromechanics Microengineering. 2013;23(12):125004.
88. Sanz-Arigita EJ, Schoonheim MM, Damoiseaux JS, Rombouts SA, Maris E, Barkhof F, et al. Loss of 'small-world'networks in Alzheimer's disease: graph analysis of FMRI resting-state functional connectivity. PLoS ONE. 2010;5(11).
89. Woodward KE, Gaxiola-Valdez I, Goodyear BG, Federico P. Frontal lobe epilepsy alters functional connections within the brain's motor network: a resting-state fMRI study. Brain connectivity. 2014;4(2):91-9.

90. Akil H, Brenner S, Kandel E, Kendler KS, King M-C, Scolnick E, et al. The future of psychiatric research: genomes and neural circuits. Science. 2010;327(5973):1580-1.
91. Bernard C, Jirsa V. Virtual Brain for neurological disease modeling. Drug Discovery Today: Disease Models. 2016;19:5-10.
92. Kaindl J, Winner B. Disease Modeling of Neuropsychiatric Brain Disorders Using Human Stem Cell-Based Neural Models. 2019.
93. Greene LA, Tischler AS. Establishment of a noradrenergic clonal line of rat adrenal pheochromocytoma cells which respond to nerve growth factor. Proceedings of the National Academy of Sciences. 1976;73(7):2424-8.
94. Huang EJ, Reichardt LF. Neurotrophins: roles in neuronal development and function. Annual review of neuroscience. 2001;24(1):677-736.
95. Vaudry D, Stork P, Lazarovici P, Eiden L. Signaling pathways for PC12 cell differentiation: making the right connections. Science. 2002;296(5573):1648-9.
96. Orlowska A, Perera PT, Al Kobaisi M, Dias A, Nguyen HKD, Ghanaati S, et al. The effect of coatings and nerve growth factor on attachment and differentiation of pheochromocytoma cells. Materials. 2018;11(1):60.
97. Malagelada C, Greene LA. PC12 cells as a model for Parkinson's disease research. Parkinson's Disease: Elsevier; 2008. p. 375-87.
98. Hu R, Cao Q, Sun Z, Chen J, Zheng Q, Xiao F. A novel method of neural differentiation of PC12 cells by using Opti-MEM as a basic induction medium. International journal of molecular medicine. 2018;41(1):195-201.
99. Chia PH, Li P, Shen K. Cellular and molecular mechanisms underlying presynapse formation. Journal of Cell Biology. 2013;203(1):11-22.
100. Marín O, Rubenstein JL. Cell migration in the forebrain. Annual review of neuroscience. 2003;26(1):441-83.
101. Gomez TM, Spitzer NC. In vivo regulation of axon extension and pathfinding by growth-cone calcium transients. Nature. 1999;397(6717):350-5.
102. Schmid RS, Anton E. Role of integrins in the development of the cerebral cortex. Cerebral cortex. 2003;13(3):219-24.
103. Arimura N, Kaibuchi K. Neuronal polarity: from extracellular signals to intracellular mechanisms. Nature Reviews Neuroscience. 2007;8(3):194-205.
104. Rasband MN. The axon initial segment and the maintenance of neuronal polarity. Nature Reviews Neuroscience. 2010;11(8):552-62.
105. Barnes AP, Polleux F. Establishment of axon-dendrite polarity in developing neurons. Annual review of neuroscience. 2009;32:347-81.
106. Madhusudanan P, Raju G, Shankarappa S. Hydrogel systems and their role in neural tissue engineering. Journal of the Royal Society Interface. 2020;17(162):20190505.
107. George J, Hsu C-C, Nguyen LTB, Ye H, Cui Z. Neural tissue engineering with structured hydrogels in CNS models and therapies. Biotechnology advances. 2019.
108. Kornev VA, Grebenik EA, Solovieva AB, Dmitriev RI, Timashev PS. Hydrogel-assisted neuroregeneration approaches towards brain injury therapy: A state-of-the-art review. Computational structural biotechnology journal. 2018;16:488-502.
109. Brännvall K, Bergman K, Wallenquist U, Svahn S, Bowden T, Hilborn J, et al. Enhanced neuronal differentiation in a three-dimensional collagen-hyaluronan matrix. Journal of neuroscience research. 2007;85(10):2138-46.

110. Lee JH, Yu H-S, Lee G-S, Ji A, Hyun JK, Kim H-W. Collagen gel three-dimensional matrices combined with adhesive proteins stimulate neuronal differentiation of mesenchymal stem cells. Journal of the Royal Society Interface. 2011;8(60):998-1010.
111. Hoban DB, Newland B, Moloney TC, Howard L, Pandit A, Dowd E. The reduction in immunogenicity of neurotrophin overexpressing stem cells after intra-striatal transplantation by encapsulation in an in situ gelling collagen hydrogel. Biomaterials. 2013;34(37):9420-9.
112. Boni R, Ali A, Shavandi A, Clarkson AN. Current and novel polymeric biomaterials for neural tissue engineering. Journal of biomedical science. 2018;25(1):90.
113. Tian W, Hou S, Ma J, Zhang C, Xu Q, Lee I, et al. Hyaluronic acid–poly-D-lysine-based three-dimensional hydrogel for traumatic brain injury. Tissue engineering. 2005;11(3-4):513-25.
114. Wang Y, Wei YT, Zu ZH, Ju RK, Guo MY, Wang XM, et al. Combination of hyaluronic acid hydrogel scaffold and PLGA microspheres for supporting survival of neural stem cells. Pharmaceutical research. 2011;28(6):1406.
115. Nisbet DR, Crompton KE, Horne MK, Finkelstein DI, Forsythe JS. Neural tissue engineering of the CNS using hydrogels. Journal of Biomedical Materials Research Part B: Applied Biomaterials: An Official Journal of The Society for Biomaterials. 2008;87(1):251-63.
116. Ashton RS, Banerjee A, Punyani S, Schaffer DV, Kane RS. Scaffolds based on degradable alginate hydrogels and poly (lactide-co-glycolide) microspheres for stem cell culture. Biomaterials. 2007;28(36):5518-25.
117. Suzuki Y, Tanihara M, Ohnishi K, Suzuki K, Endo K, Nishimura Y. Cat peripheral nerve regeneration across 50 mm gap repaired with a novel nerve guide composed of freeze-dried alginate gel. Neuroscience letters. 1999;259(2):75-8.
118. Hashimoto T, Suzuki Y, Kitada M, Kataoka K, Wu S, Suzuki K, et al. Peripheral nerve regeneration through alginate gel: analysis of early outgrowth and late increase in diameter of regenerating axons. Experimental brain research. 2002;146(3):356-68.
119. Wu S, Suzuki Y, Tanihara M, Ohnishi K, Endo K, Nishimura Y. Repair of facial nerve with alginate sponge without suturing: an experimental study in cats. Scandinavian journal of plastic reconstructive surgery and hand surgery. 2002;36(3):135-40.
120. Cooper A, Bhattarai N, Zhang M. Fabrication and cellular compatibility of aligned chitosan–PCL fibers for nerve tissue regeneration. Carbohydrate Polymers. 2011;85(1):149-56.
121. Tseng TC, Tao L, Hsieh FY, Wei Y, Chiu IM, Hsu Sh. An injectable, self-healing hydrogel to repair the central nervous system. Advanced materials. 2015;27(23):3518-24.
122. Mooney R, Tawil B, Mahoney M. Specific fibrinogen and thrombin concentrations promote neuronal rather than glial growth when primary neural cells are seeded within plasma-derived fibrin gels. Tissue Engineering Part A. 2010;16(5):1607-19.
123. Itosaka H, Kuroda S, Shichinohe H, Yasuda H, Yano S, Kamei S, et al. Fibrin matrix provides a suitable scaffold for bone marrow stromal cells transplanted into injured spinal cord: a novel material for CNS tissue engineering. Neuropathology. 2009;29(3):248-57.

124. Farzamfar S, Esmailpour F, Rahmati M, Vaez A, Mirzaii M, Garmabi B, et al. Poly-lactic Acid/Gelatin Nanofiber (PLA/GTNF) Conduits Containing Platelet-Rich Plasma for Peripheral Nerve Regeneration. International Journal of Health Studies. 2017;3(2).
125. Carriel V, Alaminos M, Garzón I, Campos A, Cornelissen M. Tissue engineering of the peripheral nervous system. Expert review of neurotherapeutics. 2014;14(3):301-18.
126. Xue C, Hu N, Gu Y, Yang Y, Liu Y, Liu J, et al. Joint use of a chitosan/PLGA scaffold and MSCs to bridge an extra large gap in dog sciatic nerve. Neurorehabilitation and neural repair. 2012;26(1):96-106.
127. Liu C, Huang Y, Pang M, Yang Y, Li S, Liu L, et al. Tissue-engineered regeneration of completely transected spinal cord using induced neural stem cells and gelatin-electrospun poly (lactide-co-glycolide)/polyethylene glycol scaffolds. PLoS ONE. 2015;10(3).
128. Lampe KJ, Mooney RG, Bjugstad KB, Mahoney MJ. Effect of macromer weight percent on neural cell growth in 2D and 3D nondegradable PEG hydrogel culture. Journal of Biomedical Materials Research Part A. 2010;94(4):1162-71.
129. Plant GW, Harvey AR, Chirila TV. Axonal growth within poly (2-hydroxyethyl methacrylate) sponges infiltrated with Schwann cells and implanted into the lesioned rat optic tract. Brain research. 1995;671(1):119-30.
130. Dalton PD, Flynn L, Shoichet MS. Manufacture of poly (2-hydroxyethyl methacrylate-co-methyl methacrylate) hydrogel tubes for use as nerve guidance channels. Biomaterials. 2002;23(18):3843-51.
131. Akhavan O, Ghaderi E, Shirazian SA, Rahighi R. Rolled graphene oxide foams as three-dimensional scaffolds for growth of neural fibers using electrical stimulation of stem cells. Carbon. 2016;97:71-7.
132. Li N, Zhang Q, Gao S, Song Q, Huang R, Wang L, et al. Three-dimensional graphene foam as a biocompatible and conductive scaffold for neural stem cells. Scientific reports. 2013;3:1604.
133. Park D-W, Schendel AA, Mikael S, Brodnick SK, Richner TJ, Ness JP, et al. Graphene-based carbon-layered electrode array technology for neural imaging and optogenetic applications. Nature communications. 2014;5:5258.
134. Kreupl F, Graham AP, Duesberg G, Steinhögl W, Liebau M, Unger E, et al. Carbon nanotubes in interconnect applications. Microelectronic Engineering. 2002;64(1-4):399-408.
135. Hopley EL, Salmasi S, Kalaskar DM, Seifalian AM. Carbon nanotubes leading the way forward in new generation 3D tissue engineering. Biotechnology advances. 2014;32(5):1000-14.
136. Imaninezhad M, Pemberton K, Xu F, Kalinowski K, Bera R, Zustiak SP. Directed and enhanced neurite outgrowth following exogenous electrical stimulation on carbon nanotube-hydrogel composites. Journal of neural engineering. 2018;15(5):056034.
137. Shah K, Vasileva D, Karadaghy A, Zustiak S. Development and characterization of polyethylene glycol–carbon nanotube hydrogel composite. Journal of Materials Chemistry B. 2015;3(40):7950-62.
138. Shin SR, Bae H, Cha JM, Mun JY, Chen Y-C, Tekin H, et al. Carbon nanotube reinforced hybrid microgels as scaffold materials for cell encapsulation. ACS nano. 2012;6(1):362-72.

139. Pohl HA. The motion and precipitation of suspensoids in divergent electric fields. Journal of Applied Physics. 1951;22(7):869-71.
140. Park K, Suk H-J, Akin D, Bashir R. Dielectrophoresis-based cell manipulation using electrodes on a reusable printed circuit board. Lab on a Chip. 2009;9(15):2224-9.
141. Ramón-Azcón J, Ahadian S, Obregón R, Camci-Unal G, Ostrovidov S, Hosseini V, et al. Gelatin methacrylate as a promising hydrogel for 3D microscale organization and proliferation of dielectrophoretically patterned cells. Lab on a Chip. 2012;12(16):2959-69.
142. Morgan H, Green NG. AC electrokinetics: Research Studies Press; 2003.
143. Hong S, Pan Q, Lee LP. Single-cell level co-culture platform for intercellular communication. Integrative biology. 2012;4(4):374-80.
144. Morgan H, Green N. AC electrokinetics: colloids and nanoparticles. 2003. Hertfordshire, England: Research Studies Press LTD.324.
145. Cao J, Cheng P, Hong F. A numerical analysis of forces imposed on particles in conventional dielectrophoresis in microchannels with interdigitated electrodes. Journal of Electrostatics. 2008;66(11-12):620-6.
146. Gagnon ZR. Cellular dielectrophoresis: applications to the characterization, manipulation, separation and patterning of cells. Electrophoresis. 2011;32(18):2466-87.
147. Ho C-T, Lin R-Z, Chang W-Y, Chang H-Y, Liu C-H. Rapid heterogeneous liver-cell on-chip patterning via the enhanced field-induced dielectrophoresis trap. Lab on a Chip. 2006;6(6):724-34.
148. Hsiung L-C, Yang C-H, Chiu C-L, Chen C-L, Wang Y, Lee H, et al. A planar interdigitated ring electrode array via dielectrophoresis for uniform patterning of cells. Biosensors and bioelectronics. 2008;24(4):869-75.
149. Suzuki M, Yasukawa T, Shiku H, Matsue T. Negative dielectrophoretic patterning with different cell types. Biosensors and bioelectronics. 2008;24(4):1043-7.
150. Tsutsui H, Yu E, Marquina S, Valamehr B, Wong I, Wu H, et al. Efficient dielectrophoretic patterning of embryonic stem cells in energy landscapes defined by hydrogel geometries. Annals of biomedical engineering. 2010;38(12):3777-88.
151. Şen M, Ino K, Ramón-Azcón J, Shiku H, Matsue T. Cell pairing using a dielectrophoresis-based device with interdigitated array electrodes. Lab on a Chip. 2013;13(18):3650-2.
152. Agarwal T, Maiti TK. Dielectrophoresis-based devices for cell patterning. Bioelectronics and Medical Devices: Elsevier; 2019. p. 493-511.
153. Yu Z, Xiang G, Pan L, Huang L, Yu Z, Xing W, et al. Negative dielectrophoretic force assisted construction of ordered neuronal networks on cell positioning bioelectronic chips. Biomedical microdevices. 2004;6(4):311-24.
154. Sebastian A, Buckle A-M, Markx GH. Formation of multilayer aggregates of mammalian cells by dielectrophoresis. Journal of Micromechanics and Microengineering. 2006;16(9):1769.
155. Albrecht DR, Tsang VL, Sah RL, Bhatia SN. Photo-and electropatterning of hydrogel-encapsulated living cell arrays. Lab on a Chip. 2005;5(1):111-8.
156. Ahadian S, Yamada S, Ramón-Azcón J, Estili M, Liang X, Nakajima K, et al. Hybrid hydrogel-aligned carbon nanotube scaffolds to enhance cardiac differentiation of embryoid bodies. Acta biomaterialia. 2016;31:134-43.

157. Ramón-Azcón J, Ahadian S, Estili M, Liang X, Ostrovidov S, Kaji H, et al. Dielectrophoretically aligned carbon nanotubes to control electrical and mechanical properties of hydrogels to fabricate contractile muscle myofibers. Advanced materials. 2013;25(29):4028-34.
158. Noble J, Munro CA, Prasad VS, Midha R. Analysis of upper and lower extremity peripheral nerve injuries in a population of patients with multiple injuries. Journal of Trauma and Acute Care Surgery. 1998;45(1):116-22.
159. Jan Y-N, Jan LY. The control of dendrite development. Neuron. 2003;40(2):229-42.
160. Millecamps S, Julien J-P. Axonal transport deficits and neurodegenerative diseases. Nature Reviews Neuroscience. 2013;14(3):161-76.
161. Cangellaris OV, Gillette MU. Biomaterials for enhancing neuronal repair. Frontiers in Materials. 2018;5:21.
162. Dang KM, Rinklin P, Schnitker J, Haberkorn B, Zobel K, Gribaudo S, et al. Fabrication of precisely aligned microwire and microchannel structures: Toward heat stimulation of guided neurites in neuronal cultures. physica status solidi. 2017;214(9):1600729.
163. Li W, Chan WWR, Ngo JCK, Lau K-F. Emerging roles of the neural adaptor FE65 in neurite outgrowth. Neural regeneration research. 2018;13(12):2085.
164. Lee S, Wang W, Hwang J, Namgung U, Min K-T. Increased ER–mitochondria tethering promotes axon regeneration. Proceedings of the National Academy of Sciences. 2019;116(32):16074-9.
165. Mirza FJ, Zahid S. The role of synapsins in neurological disorders. Neuroscience bulletin. 2018;34(2):349-58.
166. Şen M, Ino K, Shiku H, Matsue T. Accumulation and detection of secreted proteins from single cells for reporter gene assays using a local redox cycling-based electrochemical (LRC-EC) chip device. Lab on a Chip. 2012;12(21):4328-35.
167. Sikora A, Ramón-Azcón J, Sen M, Kim K, Nakazawa H, Umetsu M, et al. Microtubule guiding in a multi-walled carbon nanotube circuit. Biomedical microdevices. 2015;17(4):78.
168. Solanki A, Chueng STD, Yin PT, Kappera R, Chhowalla M, Lee KB. Axonal alignment and enhanced neuronal differentiation of neural stem cells on graphene-nanoparticle hybrid structures. Advanced Materials. 2013;25(38):5477-82.
169. Kang K, Choi SE, Jang HS, Cho WK, Nam Y, Choi IS, et al. In vitro developmental acceleration of hippocampal neurons on nanostructures of self-assembled silica beads in filopodium-size ranges. Angewandte Chemie International Edition. 2012;51(12):2855-8.

CURRICULUM VITAE

Fikri Seven
Biomedical Engineer

Email
fikrise7en@gmail.com
Address
Çamlıpınar Quarter, 254/50 Street, No:12, Buca,
İzmir, Turkey
Phone
+90 (507) 2796878
Date of birth
1995-04-13

EDUCATION

M.Sc. - Biomedical Technologies (Eng), İzmir Katip Çelebi University (2018-…)

B.Sc. - Biomedical Engineering (Eng) (3.12/4.00), İzmir Katip Çelebi University (2013-2018)

EXPERIENCES

Intern (February-June 2016, İzmir/Turkey)
İzmir Katip Çelebi University Atatürk Training and Research Hospital

Intern (June-July 2017, İzmir/Turkey)
Meditera

Laboratory Technician (October 2018-May 2020, İzmir/Turkey)
İzmir Katip Çelebi University

FOREIGN LANGUAGES

ENGLISH - ADVANCED
RUSSIAN – STARTER

CERTIFICATIONS & COURSES

- GMP - Good Manufacturing Practices Training (2020)
- GLP - Good Laboratory Practices Training (2020)
- ISO 45001 - 2018 Occupational Health and Safety Training (2020)
- ISO 13485 - 2016 Medical Devices Quality Management System Training (2020)
- ISO 9001 - 2015 Quality Management System Training (2020)
- Scientific Project Writing Techniques for Young Entrepreneurs (2016)
- Clinical Ionizing Radiation Safety Training (2016)
- Clinical Engineering Services Training in Turkey (2016)
- Biomedical Calibration and Technologies (2015)
- International Eurasian Conference On Biological And Chemical Sciences (EurasianBioChem) 2020 Participation
- National Congress of Medical Technologies (TIPTEKNO) 2019 Participation
- National Meeting of Biomedical Engineering (BİYOMUT) 2016 Participation

PUBLICATIONS

- Seven, F., Gölcez, T., Yaralı, Z. B., Onak, G., Karaman, O., & Şen, M. "Guiding neural extensions of PC12 cells on carbon nanotube tracks dielectrophoretically formed in poly (ethylene glycol) dimethacrylate." RSC Advances (2020).
- Seven F, Gölcez T, Şen M. "Nanoporous carbon-fiber microelectrodes for sensitive detection of H_2O_2 and dopamine." Journal of Electroanalytical Chemistry (2020).
- Seven F, Gölcez T, Şahinler M, Şendemir A, Karaman O, Şen M. "Prolonged Electrical Stimulation of Neuronal PC12 Cells Using a Microchip." 2019 Medical Technologies Congress (TIPTEKNO). IEEE, 2019.

CONFERENCE PRESENTATIONS

- Guiding neural extensions of PC12 cells on dielectrophoretically aligned MWCNTs in poly(ethylene glycol)dimethacrylate. EurasianBioChem 2020
- Electrical stimulation of PC12 cells for neural differentiation on monolayer graphene coated IDA-microchips. EurasianBioChem 2020
- High-sensitive detection of H_2O_2 and dopamine using thermally annealed carbon-fiber microelectrodes. EurasianBioChem 2020
- Prolonged Electrical Stimulation of Neuronal PC12 Cells Using a Microchip. TIPTEKNO 2019

PROJECT

- TUBITAK 3501 - Fabrication of a lab-on-a chip device for neural guiding (Scholarship) (October 2018-May 2020) (TUBITAK Project No: 215E003).